Digital Communications

Chapter 13 Fading Channels I: Characterization and Signaling

Po-Ning Chen, Professor

Institute of Communications Engineering
National Chiao-Tung University, Taiwan

13.1 Characterization of fading multipath channels

The multipath fading channels with additive noise

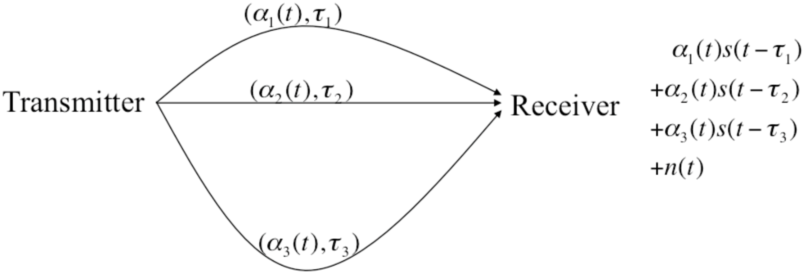

Time spread phenomenon of multipath channels

(Unpredictable) Time-variant factors

- Delay
- Number of spreads
- Size of the receive pulses

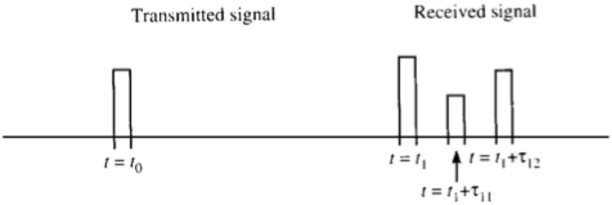

Transmitted signal

$$s(t) = \mathbf{Re}\left\{s_\ell(t)e^{\imath 2\pi f_c t}\right\}$$

Received signal in absence of additive noise

$$\begin{aligned}
r(t) &= \int_{-\infty}^{\infty} c(\tau;t)s(t-\tau)d\tau \\
&= \int_{-\infty}^{\infty} c(\tau;t)\mathbf{Re}\left\{s_\ell(t-\tau)e^{\imath 2\pi f_c(t-\tau)}\right\}d\tau \\
&= \mathbf{Re}\left\{\left(\int_{-\infty}^{\infty} c(\tau;t)e^{-\imath 2\pi f_c \tau}s_\ell(t-\tau)d\tau\right)e^{\imath 2\pi f_c t}\right\} \\
&= \mathbf{Re}\left\{\left(s_\ell(t) \star \underbrace{c(\tau;t)e^{-\imath 2\pi f_c \tau}}_{\triangleq c_\ell(\tau;t)}\right)e^{\imath 2\pi f_c t}\right\}
\end{aligned}$$

In Slide 2-28, we define the lowpass equivalent system as

$$\begin{cases} X_\ell(f) \triangleq 2X_+(f+f_0) \\ Y_\ell(f) \triangleq 2Y_+(f+f_0) \\ H_\ell(f) \triangleq 2H_+(f+f_0) \end{cases} \quad \text{and obtain} \quad \begin{cases} Y_\ell(f) = \frac{1}{2}X_\ell(f)H_\ell(f) \\ (\text{i.e., } y_\ell(f) = \frac{1}{2}x_\ell(t) \star h_\ell(t)) \end{cases}$$

Here, under a time-invariant $c(\tau;t) = c(\tau)$, we actually define

$$c_\ell(\tau) \triangleq c(\tau)e^{-\imath 2\pi f_c \tau},$$

equivalently,

$$C_\ell(f) = \int_{-\infty}^{\infty} c(\tau)e^{-\imath 2\pi f_c \tau}e^{-\imath 2\pi f \tau}\,d\tau = C(f+f_0).$$

Thus, the new "lowpass equivalence" yields

$$\begin{cases} S_\ell(f) \triangleq 2S_+(f+f_0) \\ R_\ell(f) \triangleq 2R_+(f+f_0) \\ C_\ell(f) \triangleq C(f+f_0) \end{cases} \Rightarrow \begin{cases} R_\ell(f) = S_\ell(f)C_\ell(f) \\ (\text{i.e., } r_\ell(f) = s_\ell(t) \star c_\ell(t)) \end{cases}$$

An advantage of this new equivalence is that the statistics of $c(\tau;t) = |c_\ell(\tau;t)|$ can be determined from the statistics of $c_\ell(\tau;t)$.

Note that for a time-varying system, t and τ specifically denote time argument and convolution argument, respectively!

We should perhaps write $s_\ell(t) \star c_\ell(\tau)$ and $s_\ell(t) \star c_\ell(\tau; t)$, which respectively denote:

$$s_\ell(t) \star c_\ell(\tau) = \int_{-\infty}^{\infty} c_\ell(\tau) s_\ell(t-\tau) d\tau$$

and

$$s_\ell(t) \star c_\ell(\tau; t) = \int_{-\infty}^{\infty} c_\ell(\tau; t) s_\ell(t-\tau) d\tau.$$

From the previous slide, we know

$$\boxed{c_\ell(\tau; t) = c(\tau; t) e^{-\imath 2\pi f_c \tau} \text{ and } c(\tau; t) = \left| c_\ell(\tau; t) \right|.}$$

Rayleigh and Rician

Measurements suggest that in certain environment, $c(\tau; t) = |c_\ell(\tau; t)| \geq 0$ can be Rayleigh distributed or Rician distributed. As a consequence, such $c(\tau; t)$ can be modeled by letting $c_\ell(\tau; t)$ be a 2-D Gaussain random process in t (not in τ).

- If $c_\ell(\tau; t)$ zero mean, $c(\tau; t) = |c_\ell(\tau; t)|$ is Rayleigh distributed. The channel $c(\tau; t)$ is said to be a Rayleigh fading channel.

- If $c_\ell(\tau; t)$ nonzero mean, $c(\tau; t) = |c_\ell(\tau; t)|$ is Rician distributed. The channel $c(\tau; t)$ is said to be a Rician fading channel.

When diversity technique is used, $c(\tau; t) = |c_\ell(\tau; t)|$ is well modeled by Nakagami m-distribution.

13.1-1 Channel correlation functions and power spectra

Assumption (WSS)

$c_\ell(\tau; t)$ is WSS in t.

$$R_{c_\ell}(\bar{\tau}, \tau; \Delta t) = \mathbb{E}\{c_\ell(\bar{\tau}; t + \Delta t) c_\ell^*(\tau; t)\}$$

is only a function of time difference Δt.

Assumption (Uncorrelated scattering or US of a WSS channel)

For $\bar{\tau} \neq \tau$, $c_\ell(\bar{\tau}; t_1)$ and $c_\ell(\tau; t_2)$ are uncorrelated for any t_1, t_2.

- τ is the convolution argument and actually represents the delay for a certain path.

Assumption (Math definition of US)

$$R_{c_\ell}(\bar{\tau}, \tau; \Delta t) = R_{c_\ell}(\tau; \Delta t)\delta(\bar{\tau} - \tau)$$

Multipath intensity profile of a WSSUS channel

- The **multipath intensity profile** or **delay power spectrum** for a WSSUS multipath fading channel is given by:

$$R_{c_\ell}(\tau) \;=\; R_{c_\ell}(\tau; \Delta t = 0)\,.$$

  - It can be interpreted as the average power output of the channel as a function of the path delay τ.

$$\mathbb{E}[|r_\ell(t)|^2] = \mathbb{E}\left[\int_{-\infty}^{\infty} c_\ell(\bar{\tau};t)s_\ell(t-\bar{\tau})d\bar{\tau}\int_{-\infty}^{\infty} c_\ell^*(\tau;t)s_\ell^*(t-\tau)d\tau\right]$$

$$= \int_{-\infty}^{\infty}\int_{-\infty}^{\infty}\mathbb{E}\big[c_\ell(\bar{\tau};t)c_\ell^*(\tau;t)\big]\mathbb{E}[s_\ell(t-\bar{\tau})s_\ell^*(t-\tau)]d\bar{\tau}d\tau$$

$$= \int_{-\infty}^{\infty}\int_{-\infty}^{\infty} R_{c_\ell}(\tau;0)\delta(\bar{\tau}-\tau)\mathbb{E}[s_\ell(t-\bar{\tau})s_\ell^*(t-\tau)]d\bar{\tau}d\tau$$

$$= \int_{-\infty}^{\infty} R_{c_\ell}(\tau;0)\mathbb{E}[|s_\ell(t-\tau)|^2]d\tau = \int_{-\infty}^{\infty} R_{c_\ell}(\tau)\mathbb{E}[|s_\ell(t-\tau)|^2]d\tau$$

Multipath spread of a WSSUS channel

- **multipath spread** or **delay spread** of a WSSUS multipath fading channel
  - **multipath spread** is the range of τ over which $R_{c_\ell}(\tau)$ is essentially non-zero; it is usually denoted by T_m.

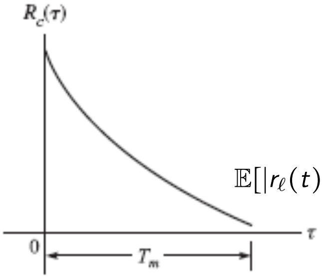

FIGURE 13.1–2
Multipath intensity profile.

$$\mathbb{E}[|r_\ell(t)|^2] \approx \int_0^{T_m} R_\ell(\tau)\mathbb{E}[|s_\ell(t-\tau)|^2]d\tau$$

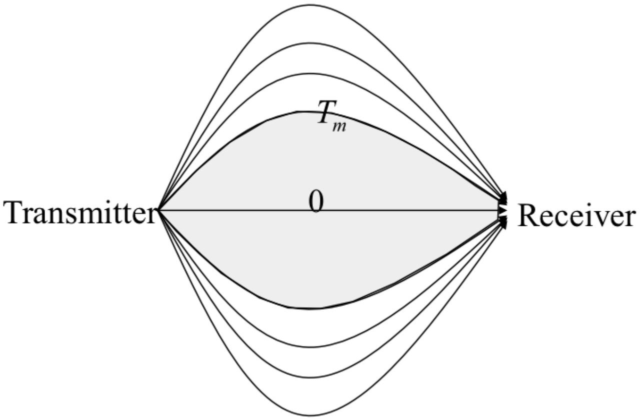

- Each τ corresponds to one path.
- No Tx power will essentially remain at Rx for paths with delay $\tau > T_m$.

Transfer function of a multipath fading channel

The transfer function of a channel impulse response $c_\ell(\tau; t)$ is the Fourier transform with respect to the convolutional argument τ:

$$\mathbf{C}_\ell(f; t) = \int_{-\infty}^{\infty} c_\ell(\tau; t) e^{-\imath 2\pi f \tau} \, d\tau$$

Property: If $c_\ell(\tau; t)$ is WSS, so is $\mathbf{C}_\ell(f; t)$.

The autocorrelation function of WSS $\mathbf{C}_\ell(f; t)$ is equal to:

$$R_{\mathbf{C}_\ell}(\bar{f}, f; \Delta t) = \mathbb{E}\left\{\mathbf{C}_\ell(\bar{f}; t + \Delta t)\mathbf{C}_\ell^*(f; t)\right\}$$

With an additional US assumption,

$$
\begin{aligned}
& R_{\mathbf{C}_\ell}(\bar{f}, f; \Delta t) \\
&= \mathbb{E}\left\{\mathbf{C}_\ell(\bar{f}; t+\Delta t)\mathbf{C}_\ell^*(f; t)\right\} \\
&= \mathbb{E}\left\{\int_{-\infty}^{\infty} c_\ell(\bar{\tau}; t+\Delta t) e^{-\imath 2\pi \bar{f}\bar{\tau}}\, d\bar{\tau} \int_{-\infty}^{\infty} c_\ell^*(\tau; t) e^{\imath 2\pi f\tau}\, d\tau\right\} \\
&= \int_{-\infty}^{\infty}\int_{-\infty}^{\infty} R_{c_\ell}(\tau; \Delta t)\delta(\bar{\tau}-\tau) e^{\imath 2\pi (f\tau - \bar{f}\bar{\tau})}\, d\tau d\bar{\tau} \\
&= \int_{-\infty}^{\infty} R_{c_\ell}(\tau; \Delta t)\, e^{-\imath 2\pi(\bar{f}-f)\tau}\, d\tau \\
&= R_{\mathbf{C}_\ell}(\Delta f; \Delta t), \text{ where } \Delta f = \bar{f} - f.
\end{aligned}
$$

For a WSSUS multipath fading channel,

$$R_{\mathbf{C}_\ell}(\Delta f; \Delta t) = \mathbb{E}\left\{\mathbf{C}_\ell(f+\Delta f; t+\Delta t)\mathbf{C}_\ell^*(f; t)\right\}$$

This is often called **spaced-frequency, spaced-time correlation function** of a WSSUS channel.

Note that $\mathrm{R}_\ell(f) \neq \mathrm{S}_\ell(f)\mathbf{C}_\ell(f;t)$, where

$$\mathrm{R}_\ell(f) = \int_{-\infty}^{\infty} r_\ell(t) e^{-\imath 2\pi f t} dt \text{ and } \mathrm{S}_\ell(f) = \int_{-\infty}^{\infty} s_\ell(t) e^{-\imath 2\pi f t} dt.$$

We only have

$$\begin{aligned}
r_\ell(t) &= \int_{-\infty}^{\infty} c_\ell(\tau;t) s_\ell(t-\tau) d\tau \\
&= \int_{-\infty}^{\infty} \left(\int_{-\infty}^{\infty} \mathbf{C}_\ell(f;t) e^{\imath 2\pi f \tau} d\tau \right) s_\ell(t-\tau) d\tau \\
&= \int_{-\infty}^{\infty} \left(\int_{-\infty}^{\infty} s_\ell(t-\tau) e^{\imath 2\pi f \tau} d\tau \right) \mathbf{C}_\ell(f;t) df \\
&= \int_{-\infty}^{\infty} \left(\int_{-\infty}^{\infty} s_\ell(u) e^{\imath 2\pi f (t-u)} d\tau \right) \mathbf{C}_\ell(f;t) df \quad (\text{Let } u = t-\tau) \\
&= \int_{-\infty}^{\infty} \mathrm{S}_\ell(f)\mathbf{C}_\ell(f;t) e^{\imath 2\pi f t} df
\end{aligned}$$

Coherent bandwidth

Summarize from the last equality of the previous derivation (in red):
$R_{\mathbf{C}_\ell}(\Delta f;\Delta t) = \int_{-\infty}^{\infty} R_{c_\ell}(\tau;\Delta t)\, e^{-\imath 2\pi(\Delta f)\tau}\, d\tau$

For the case of $\Delta t = 0$, we have

$$\underbrace{R_{\mathbf{C}_\ell}(\Delta f)}_{\substack{\text{spaced-frequency}\\ \text{correlation function}}} = \int_{-\infty}^{\infty} R_{c_\ell}(\tau)\, e^{-\imath 2\pi(\Delta f)\tau}\, d\tau$$

- Recall that $R_{c_\ell}(\tau) = 0$ outside $[0, T_m)$.
- $(\Delta f)_c = \frac{1}{T_m}$ is called coherent bandwidth.
- From Slide 13-11, $\mathbb{E}[|r_\ell(t)|^2] = \int_{-\infty}^{\infty} R_{c_\ell}(\tau)\mathbb{E}[|s_\ell(t-\tau)|^2]d\tau$

$$\Rightarrow \int_{-\infty}^{\infty} \mathbb{E}[|r_\ell(t)|^2]e^{-\imath 2\pi(\Delta f)t}dt = R_{\mathbf{C}_\ell}(\Delta f) \int_{-\infty}^{\infty} \mathbb{E}[|s_\ell(t)|^2]e^{-\imath 2\pi(\Delta f)t}dt$$

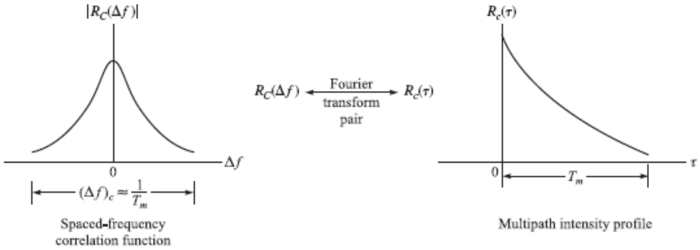

FIGURE 13.1–3
Relationship between $R_C(\Delta f)$ and $R_c(\tau)$.

Example.

Give $R_{c_\ell}(\tau) = 10^7(10^{-7} - \tau)$ for $0 \le \tau < 100$ ns. Then,

$$R_{\mathbf{C}_\ell}(\Delta f) = \frac{10^7}{4\pi^2(\Delta f)^2}\left(e^{-\imath 2\pi\cdot 10^{-7}\cdot\Delta f} - 1\right) - \frac{1}{2\pi\Delta f}\imath\,.$$

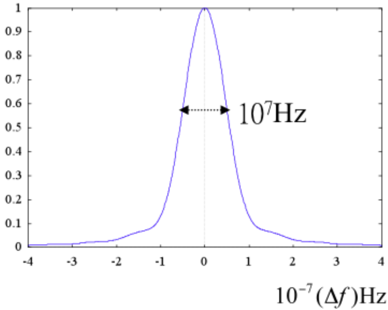

$$\frac{|R_{\mathbf{C}_\ell}(\Delta f)|}{|R_{\mathbf{C}_\ell}(0)|}$$

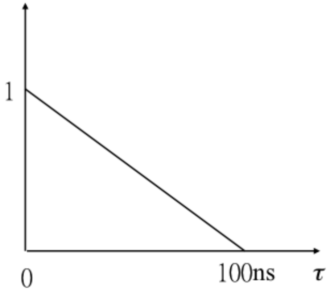

$R_{c_\ell}(\tau)$

Coherent bandwidth

$$R_{\mathbf{C}_\ell}(\bar{f}, f; 0) = \mathbb{E}\left\{\mathbf{C}_\ell(\bar{f}; t)\mathbf{C}_\ell^*(f; t)\right\} \text{ and } r_\ell(t) = \int_{-\infty}^{\infty} \mathrm{S}_\ell(f)\mathbf{C}_\ell(f; t)e^{\imath 2\pi f t} df$$

If $\bar{f} - f > (\Delta f)_c$, $R_{\mathbf{C}_\ell}(\bar{f}, f; 0)$ will be essentially small (nearly uncorrelated or nearly independent if Gaussian).

Thus, two sinusoids $\mathrm{S}_\ell(\bar{f})$ and $\mathrm{S}_\ell(f)$ with frequency separation greater than $(\Delta f)_c$ are respectively multiplied by nearly independent $\mathbf{C}_\ell(\bar{f}; t)$ and $\mathbf{C}_\ell(f; t)$ and hence are affected very differently by the channel.

If signal transmitted bandwidth $B > (\Delta f)_c$, the channel is called **frequency selective**.

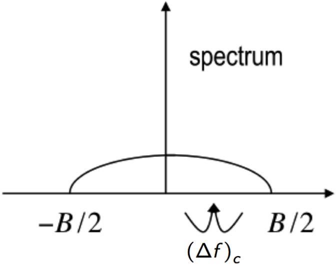

If signal transmitted bandwidth $B < (\Delta f)_c$, the channel is called **frequency non-selective**.

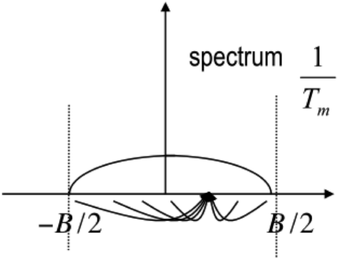

- For frequency selective channels, the signal shape is more severely distorted than that of frequency non-selective channels.

- Criterion for frequency selectivity:

$$B > (\Delta f)_c \quad \Leftrightarrow \quad \frac{1}{T} > \frac{1}{T_m} \quad \Leftrightarrow \quad T < T_m.$$

Time varying characterization: Doppler

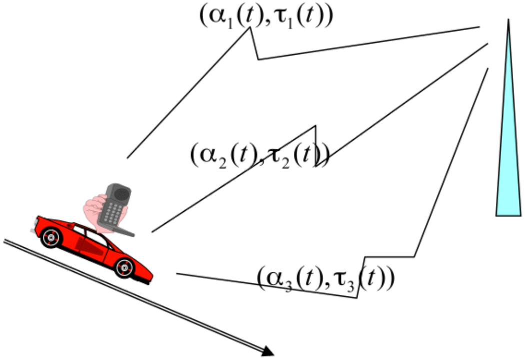

Doppler effect appears via the argument Δt.

The Doppler power spectrum is

$$S_{\mathbf{C}_\ell}(\lambda) = \int_{-\infty}^{\infty} R_{\mathbf{C}_\ell}(\Delta f = 0; \Delta t) e^{-\imath 2\pi\lambda(\Delta t)} d(\Delta t),$$

where λ is referred to as the **Doppler frequency**.

- B_d = Doppler spread is the range such that $S_{\mathbf{C}_\ell}(\lambda)$ is essentially zero.
- $(\Delta t)_c = \frac{1}{B_d}$ is called the coherent time.
- If symbol period $T > (\Delta t)_c$, the channel is classified as **Fast Fading**.
    - I.e., channel statistics changes within one symbol!
- If symbol period $T < (\Delta t)_c$, the channel is classified as **Slow Fading**.

Operational Characteristic of $S_{\mathbf{C}_\ell}(\lambda)$

We can obtain as similarly from Slide 13-11 that

$$\begin{aligned}
\bar{R}_{r_\ell}(\Delta t) &= \lim_{T\to\infty}\frac{1}{2T}\int_{-T}^{T}\mathbb{E}[r_\ell(t+\Delta t)r_\ell^*(t)]dt \\
&= \lim_{T\to\infty}\frac{1}{2T}\int_{-T}^{T}\int_{-\infty}^{\infty}\int_{-\infty}^{\infty} R_{c_\ell}(\tau;\Delta t)\delta(\bar{\tau}-\tau) \\
&\qquad \times\mathbb{E}[s_\ell(t+\Delta t-\bar{\tau})s_\ell^*(t-\tau)]d\bar{\tau}d\tau dt \\
&= \lim_{T\to\infty}\frac{1}{2T}\int_{-T}^{T}\int_{-\infty}^{\infty} R_{c_\ell}(\tau;\Delta t)\mathbb{E}[s_\ell(t+\Delta t-\tau)s_\ell^*(t-\tau)]d\tau dt \\
&= \int_{-\infty}^{\infty} R_{c_\ell}(\tau;\Delta t)\bar{R}_{s_\ell}(\Delta t)d\tau \\
&= R_{\mathbf{C}_\ell}(\Delta f=0;\Delta t)\bar{R}_{s_\ell}(\Delta t)
\end{aligned}$$

$$\Rightarrow \bar{S}_{r_\ell}(\lambda) = S_{\mathbf{C}_\ell}(\lambda)\star\bar{S}_{s_\ell}(\lambda).$$

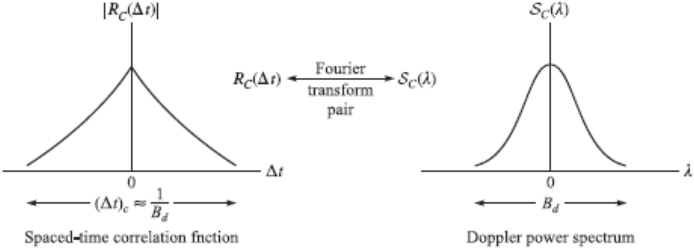

FIGURE 13.1–4
Relationship between $R_C(\Delta t)$ and $\mathcal{S}_C(\lambda)$.

Summary:

$R_{c_\ell}(\tau;\Delta t)$ Channel autocorrelation function

$$\text{1-D FT: } \begin{cases} R_{\mathbf{C}_\ell}(\Delta f;\Delta t) = \mathcal{F}_\tau\left\{R_{c_\ell}(\tau;\Delta t)\right\} & \text{Spaced-freq spaced-time correlation func} \\ S(\tau;\lambda) = \mathcal{F}_{\Delta t}\left\{R_{c_\ell}(\tau;\Delta t)\right\} & \text{Scattering function} \end{cases}$$

$$\text{2D FT: } S_{\mathbf{C}_\ell}(\Delta f;\lambda) = \mathcal{F}_{\tau,\Delta t}\left\{R_{c_\ell}(\tau;\Delta t)\right\}$$ Doppler power spectrum ($\Delta f = 0$)

$R_{\mathbf{C}_\ell}(\Delta f;\Delta t)$ Spaced-freq spaced-time correlation function

$$\text{1-D FT: } \begin{cases} R_{c_\ell}(\tau;\Delta t) = \mathcal{F}^{-1}_{\Delta f}\left\{R_{\mathbf{C}_\ell}(\Delta f;\Delta t)\right\} & \text{Chan autocorr func} \\ S_{\mathbf{C}_\ell}(\Delta f;\lambda) = \mathcal{F}_{\Delta t}\left\{R_{\mathbf{C}_\ell}(\Delta f;\Delta t)\right\} & \text{Doppler power spectrum } (\Delta f = 0) \end{cases}$$

$$\text{2D FT: } S(\tau;\lambda) = \mathcal{F}^{-1}_{\Delta f}\mathcal{F}_{\Delta t}\left\{R_{\mathbf{C}_\ell}(\Delta f;\Delta t)\right\}$$ Scattering function

Scattering function

- The scattering function can be used to identify both "delay spread" and "Doppler spread."

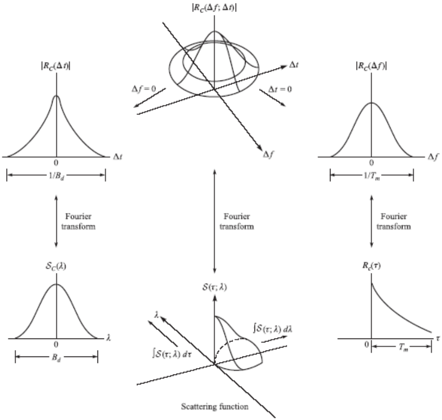

FIGURE 13.1–5
Relationships among the channel correlation functions and power spectra. [*From Green (1962), with permission.*]

Example. Medium-range tropospheric scatter channel

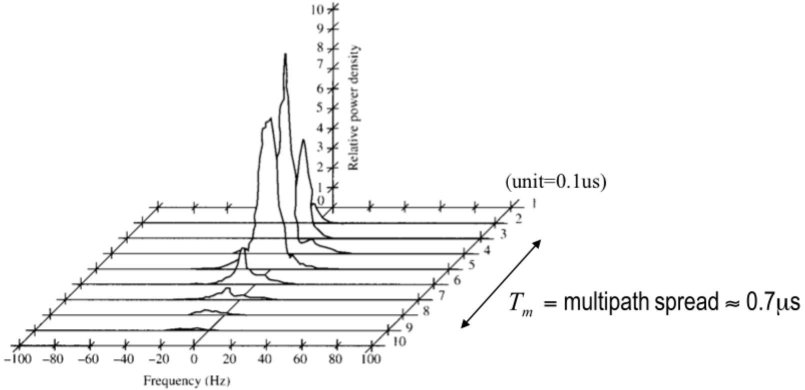

Scattering function of a medium-range tropospheric scatter channel. The taps delay increment is 0.1 μs.

$$\longleftrightarrow\; B_d = \text{Doppler spread, varies with paths}$$

$$= \text{(often) 3dB bandwidth} \approx 1\text{Hz} \sim 30\text{Hz}$$

Example study of delay spread

The **median delay spread** is the 50% value, meaning that 50% of all channels has a delay spread that is lower than the median value. Clearly, the median value is not so interesting for designing a wireless link, because you want to guarantee that the link works for at least 90% or 99% of all channels. Therefore the second column gives the measured **maximum delay spread** values. The reason to use maximum delay spread instead of a 90% or 99% value is that many papers only mention the maximum value. From the papers that do present cumulative distribution functions of their measured delay spreads, it can be deduced that the 99% value is only a few percent smaller than the maximum delay spread.

Measured delay spreads in frequency range of 800M to 1.5 GHz (surveyed by Richard van Nee, Lucent Technologies, Nov. 1997)

Median Delay Spread [ns]	Maximum Delay Spread [ns]	Remarks
25	50	Office building
30	56	Office building
27	43	Office building
11	58	Office building
35	80	Office building
40	90	Shopping mall
80	120	Airport
120	180	Factory
50	129	Warehouse
120	300	Factory

Measured delay spreads in frequency range of 1.8 GHz to 2.4 GHz (surveyed by Richard van Nee)

Median Delay Spread [ns]	Maximum Delay Spread [ns]	Remarks
40	120	Large building (New York stock exchange)
40	95	Office building
40	150	Office building
60	200	Shopping center
106	270	Laboratory
19	30	Office building: single room only
20	65	Office building
30	75	Canteen
105	170	Shopping center
30	56	Office building
25	30	Office building: single room only

Measured delay spreads in frequency range of 4 GHz to 6 GHz (surveyed by Richard van Nee)

Median Delay Spread [ns]	Maximum Delay Spread [ns]	Remarks
40	120	Large building (New York stock exchange)
50	60	Office building
35	55	Meeting room (5mx5m) with metal walls
10	35	Single room with stone walls
40	130	Office building
40	120	Indoor sports arena
65	125	Factory
25	65	Office building
20	30	Office building: single room only

Conclusion by Richard van Nee: Measurements done at different frequencies show the multipath channel characteristics are almost the same from 1 to 5 GHz.

Jakes' model: Example 13.1-3

Jakes' model

- A widely used model for Doppler power spectrum is the so-called Jakes' model (Jakes, 1974)

$$R_{\mathbf{c}_\ell}(\Delta t) = J_0(2\pi f_m \cdot \Delta t)$$

and

$$S_{\mathbf{c}_\ell}(\lambda) = \begin{cases} \frac{1}{\pi f_m} \frac{1}{\sqrt{1-(\lambda/f_m)^2}}, & |\lambda| \le f_m \\ 0, & \text{otherwise} \end{cases}$$

where

$$\begin{cases} f_m = (v/c) f_c \text{ is the maximum Doppler shift} \\ v \text{ is the vehicle speed (m/s)} \\ c \text{ is the light speed } (3 \times 10^8 \text{ m/s}) \\ f_c \text{ is the carrier frequency} \\ J_0(\cdot) \text{ is the zero-order Bessel function} \\ \qquad \text{of the first kind.} \end{cases}$$

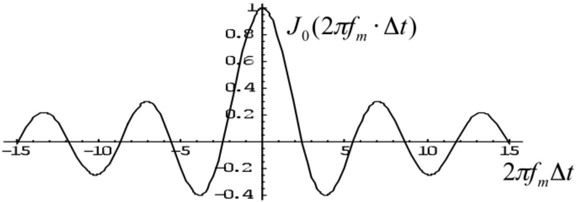
$J_0(2\pi f_m \cdot \Delta t)$
1
0.8
0.6
0.4
0.2
−0.2
−0.4
−15
−10
−5
5
10
15
$2\pi f_m \Delta t$

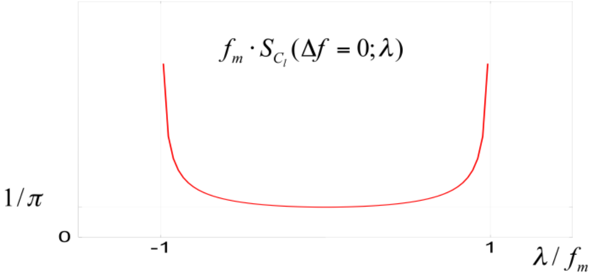
$f_m \cdot S_{C_l}(\Delta f = 0; \lambda)$
$1/\pi$
0
-1
1
λ / f_m

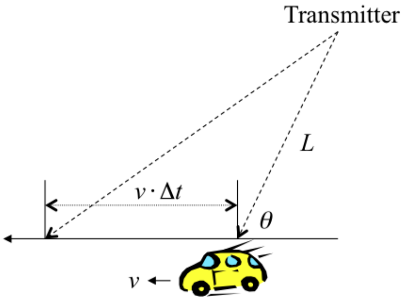

- Difference in path length

$$
\begin{aligned}
\Delta L &= \sqrt{(L\sin(\theta))^2 + (L\cos(\theta) + v\cdot\Delta t)^2} - L \\
&= \sqrt{L^2 + v^2(\Delta t)^2 + 2L\cdot v\cdot\Delta t\cdot\cos(\theta)} - L
\end{aligned}
$$

- Phase change $\Delta\phi = 2\pi\frac{\Delta L}{(c/f_c)}$ $\left(= 2\pi\frac{\Delta L}{\text{wavelength}}\right)$

- Estimated Doppler shift

$$\begin{aligned}
\lambda_m &= \lim_{\Delta t \to 0} \frac{1}{2\pi} \frac{\Delta \phi}{\Delta t} \\
&= \frac{1}{c/f_c} \lim_{\Delta t \to 0} \frac{\sqrt{L^2 + v^2(\Delta t)^2 + 2L \cdot v \cdot \Delta t \cdot \cos(\theta)} - L}{\Delta t} \\
&= \frac{v f_c}{c} \cos(\theta) = f_m \cos(\theta)
\end{aligned}$$

Example. $v = 108$ km/hour, $f_c = 5$ GHz and $c = 1.08 \times 10^9$ km/hour.

$$\Longrightarrow \lambda_m = 500 \cos(\theta) \text{ Hz.}$$

Notably, $\frac{500 \text{ Hz}}{5GHz} = 0.1$ ppm.

Jakes' model

Here, a rough derivation is provided for Jakes' model.

Just to give you a rough idea of how this model is obtained.

Suppose $\tau = \tau(t)$ is the delay of some path.

$$\tau'(t) = \lim_{\Delta t \to 0} \frac{\tau(t+\Delta t) - \tau(t)}{\Delta t}$$
$$= \lim_{\Delta t \to 0} \frac{\frac{L+\Delta L}{c} - \frac{L}{c}}{\Delta t}$$
$$= \lim_{\Delta t \to 0} \frac{\Delta L}{c \Delta t}$$
$$= \frac{v}{c} \cos(\theta)$$

$$\Rightarrow \tau(t) \approx \frac{v}{c} \cos(\theta)\ t + \tau_0$$

(Assume for simplicity $\tau_0 = 0$.)

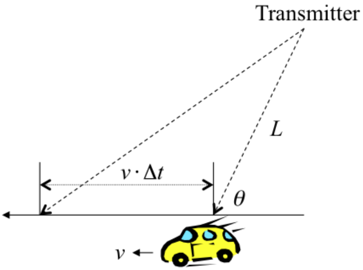

Assume that $c(\tau;t) \approx a\cdot\delta(\tau-\tau(t))$, a constant-attenuation single-path system. Then

$$
\begin{aligned}
c_\ell(\tau;t) = c(\tau;t)e^{-\imath 2\pi f_c\tau} & \\
&\approx \quad a\cdot\delta(\tau-\tau(t))e^{-\imath 2\pi f_c\cdot\tau(t)} \\
&= \quad a\cdot\delta(\tau-(v/c)\cos(\theta)t)e^{-\imath 2\pi f_c\left(\frac{v}{c}\cos(\theta)t\right)} \\
&= \quad a\cdot\delta(\tau-(f_m/f_c)\cos(\theta)t)e^{-\imath 2\pi f_m\cos(\theta)t}
\end{aligned}
$$

and

$$
\begin{aligned}
&R_{c_\ell}(\tau;t+\Delta t,t) \\
&= \int_{-\infty}^{\infty}\mathbb{E}\left[c_\ell(\bar\tau;t+\Delta t)c_\ell^*(\tau;t)\right]d\bar\tau \\
&= \int_{-\infty}^{\infty}\mathbb{E}\Big[a\cdot\delta(\bar\tau-(f_m/f_c)\cos(\theta)(t+\Delta t))e^{-\imath 2\pi f_m\cos(\theta)(t+\Delta t)} \\
&\qquad\qquad \cdot a\cdot\delta(\tau-(f_m/f_c)\cos(\theta)t)e^{\imath 2\pi f_m\cos(\theta)t}\Big]d\bar\tau \\
&= a^2\cdot\mathbb{E}\left[e^{-\imath 2\pi f_m\cos(\theta)\cdot\Delta t}\right]\delta(\tau-(f_m/f_c)\cos(\theta)t)
\end{aligned}
$$

$$
\begin{aligned}
& R_{\mathsf{C}_\ell}(\Delta f = 0; t+\Delta t, t) \quad \left(= \int_{-\infty}^{\infty} R_{c_\ell}(\tau; t+\Delta t, t) e^{\imath 2\pi(\Delta f)\tau} d\tau \Big|_{\Delta f = 0} \right) \\
= \quad & \int_{-\infty}^{\infty} R_{c_\ell}(\tau; t+\Delta t, t) d\tau \\
= \quad & \int_{-\infty}^{\infty} a^2 \cdot \mathbb{E}\left[e^{-\imath 2\pi f_m \cos(\theta)\cdot\Delta t} \right] \delta(\tau - (f_m/f_c)\cos(\theta) t) d\tau \\
= \quad & a^2 \cdot \mathbb{E}\left[e^{-\imath 2\pi f_m \cos(\theta)\cdot\Delta t} \right] \\
= \quad & J_0(2\pi f_m \cdot \Delta t) \quad \left(= R_{\mathsf{C}_\ell}(\Delta f = 0; \Delta t) \right)
\end{aligned}
$$

where the last step is valid if θ uniformly distributed over $[-\pi, \pi)$, and $a = 1$.

θ can be treated as uniformly distributed over $[-\pi, \pi)$ and independent of attenuation α and delay path τ.

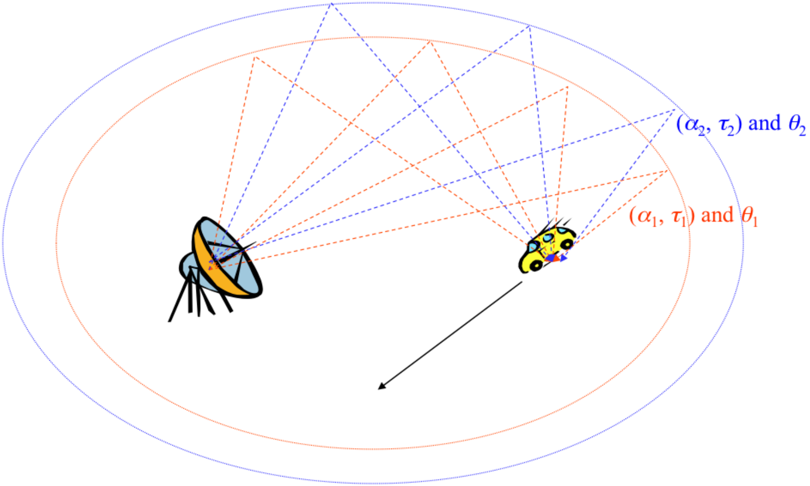

Channel model from IEEE 802.11 Handbook

- A consistent channel model is required to allow comparison among different WLAN systems.[1]

- The IEEE 802.11 Working Group adopted the following channel model as the baseline for predicting multipath for modulations used in IEEE 802.11a and IEEE 802.11b, which is ideal for software simulations.

  - The phase is uniformly distributed.

  - The magnitude is Rayleigh distributed with average power decaying exponentially.

---

[1] B. O'Hara and A. Petrick, *IEEE 802.11 Handbook: A Designer's Companion*, pp. 164–166, IEEE Press,1999

Time Invariant: $c_\ell(\tau;t) = c_\ell(\tau) = \sum_{i=0}^{i_{\max}-1} \alpha_i e^{-\imath\phi_i}\delta(\tau - iT_s)$

$$\text{where } \begin{cases} T_s \text{ sampling period} \\ \alpha_i e^{\imath\phi_i} \equiv \mathcal{N}(0,\sigma_i^2/2) + \imath\mathcal{N}(0,\sigma_i^2/2) \\ \sigma_i^2 = \sigma_0^2 e^{-iT_s/\tau_{\text{rms}}} \\ \sigma_0^2 = 1 - e^{-T_s/\tau_{\text{rms}}} \quad \left(\text{Thus } \sum_{i=0}^{\infty}\sigma_i^2 = 1\right) \end{cases}$$

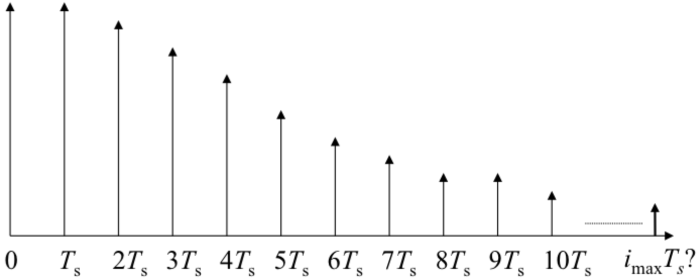

$$
\begin{aligned}
R_{c_\ell}(\tau) &= \int_{-\infty}^{\infty} \mathbb{E}\left[c_\ell(\bar\tau;t)c_\ell^*(\tau;t)\right]d\bar\tau = \int_{-\infty}^{\infty} \mathbb{E}\left[c_\ell(\bar\tau)c_\ell^*(\tau)\right]d\bar\tau \\
&= \sum_{i=0}^{i_{\max}-1}\int_{-\infty}^{\infty}\mathbb{E}\left[\alpha_i^2\right]\delta(\tau-iT_s)\delta(\bar\tau-\tau)d\bar\tau \\
&= \sum_{i=0}^{i_{\max}-1}\mathbb{E}\left[\alpha_i^2\right]\delta(\tau-iT_s) \\
&= \sum_{i=0}^{i_{\max}-1}\sigma_0^2 e^{-iT_s/\tau_{\text{rms}}}\delta(\tau-iT_s)
\end{aligned}
$$

By this example, I want to introduce the rms delay spread. By definition, the "effective" rms delay is

$$
\begin{aligned}
T_{\text{rms}}^2 &= \frac{\int_{-\infty}^{\infty}\tau^2 R_{c_\ell}(\tau)d\tau}{\int_{-\infty}^{\infty}R_{c_\ell}(\tau)d\tau} - \left(\frac{\int_{-\infty}^{\infty}\tau R_{c_\ell}(\tau)d\tau}{\int_{-\infty}^{\infty}R_{c_\ell}(\tau)d\tau}\right)^2 \\
&= \frac{\sum_{i=0}^{i_{\max}-1}(iT_s)^2\cancel{\sigma_0^2}e^{-iT_s/\tau_{\text{rms}}}}{\sum_{i=0}^{i_{\max}-1}\cancel{\sigma_0^2}e^{-iT_s/\tau_{\text{rms}}}} - \left(\frac{\sum_{i=0}^{i_{\max}-1}(iT_s)\cancel{\sigma_0^2}e^{-iT_s/\tau_{\text{rms}}}}{\sum_{i=0}^{i_{\max}-1}\cancel{\sigma_0^2}e^{-iT_s/\tau_{\text{rms}}}}\right)^2
\end{aligned}
$$

We wish to choose $i_{\max}$ such that $T_{\text{rms}} \approx \tau_{\text{rms}}$.

Let $\tilde{\tau}_{\text{rms}} = \frac{\tau_{\text{rms}}}{T_s}$ and $\tilde{T}_{\text{rms}} = \frac{T_{\text{rms}}}{T_s}$.

These unit-less terms $\tilde{\tau}_{\text{rms}}$ and $\tilde{T}_{\text{rms}}$ are usually ≥ 1.

$$
\begin{aligned}
\tilde{T}^2_{\text{rms}} &= \frac{\sum_{i=0}^{n-1} i^2 p^i}{\sum_{i=0}^{n-1} p^i} - \left(\frac{\sum_{i=0}^{n-1} i p^i}{\sum_{i=0}^{n-1} p^i}\right)^2 \quad \text{with } p = e^{-1/\tilde{\tau}_{\text{rms}}} = e^{-x} \text{ and } n = i_{\max} \\
&= \frac{p}{(1-p)^2} - \frac{n^2 p^n}{(1-p^n)^2} \quad (\text{Note } p^n = e^{-nx}.) \\
&= \left(\frac{1}{x^2} - \frac{1}{12} + \frac{x^2}{240} + \cdots\right) - \left(\frac{(nx)^2 e^{-nx}}{(1-e^{-nx})^2}\right)\frac{1}{x^2} \approx \tilde{\tau}^2_{\text{rms}} = \frac{1}{x^2}
\end{aligned}
$$

where Taylor expansion yields $\frac{x^2 p}{(1-p)^2} = \frac{x^2 e^{-x}}{(1-e^{-x})^2} = 1 - \frac{x^2}{12} + \frac{x^4}{240} + O(x^8)$.

$$
\frac{(nx)^2 e^{-nx}}{(1-e^{-nx})^2} \leq 0.01 \Rightarrow nx \geq 9 \Rightarrow i_{\max} = n \geq \frac{9}{x} = 9\tilde{\tau}_{\text{rms}} = 9\frac{\tau_{\text{rms}}}{T_s}
$$

The Handbook suggests $i_{\max} = 10$.

Typical multipath delay spread for indoor environment (Table 8-1 in IEEE 802.11 Handbook) with $T_s = 1/(20 \times 10^6) = 50$ nsec.

Environment	Delay Spread	$\tilde{\tau}_{\text{rms}}$	i_{max}	$\tilde{T}_{\text{rms}}$
Home	<50 nsec	1	10	0.957
Office	~ 100 nsec	2	20	1.975
Manufacturing floor	200–300 nsec	4–6	40–60	3.980–5.980

13.1-2 Statistical models for fading channels

In addition to zero-mean Gaussian (Rayleigh), non-zero-mean Gaussian (Rice) and Nakagami-m distributions, there are other models for $c_\ell(\tau; t)$ proposed in the literature.

Example.

- Channels with a direct path and a single multipath component, such as airplane-to-ground communications

$$c_\ell(\tau; t) = \alpha\delta(\tau) + \beta(t)\delta(\tau - \tau_0(t))$$

  where α controls the power in the direct path and is named *specular component*, and $\beta(t)$ is modeled as zero-mean Gaussian.

Example.

- Microwave LOS radio channels used for long-distance voice and video transmission by telephone companies in the 6 GHz band (Rummler 1979)

$$c_\ell(\tau) = \alpha\left[\delta(\tau) - \beta e^{\imath 2\pi f_0 \tau}\delta(\tau - \tau_0)\right]$$

where

$$\begin{cases} \alpha & \text{overall attenuation parameter} \\ \beta & \text{shape parameter due to multipath components} \\ \tau_0 & \text{time delay} \\ f_0 & \text{frequency of the fade minimum, i.e.,} \end{cases}$$

$f_0 = \arg\min_{f\in\mathbb{R}} |\mathbf{C}_\ell(f)| = \arg\min_{f\in\mathbb{R}} \left|1 - \beta e^{-\imath 2\pi(f-f_0)\tau_0}\right|$
and $\mathrm{R}_\ell(f_0) = \mathrm{S}_\ell(f_0)\mathbf{C}_\ell(f_0) = \mathrm{S}_\ell(f_0)\alpha(1-\beta)$.

Rummler found that

1. $\alpha \perp \beta$ (Independent)
2. $f(\beta) \approx (1-\beta)^{2.3}$ (pdf)
3. $-\log(\alpha)$ Gaussian distributed (i.e., α lognormal distributed)
4. $\tau_0 \approx 6.3$ ns

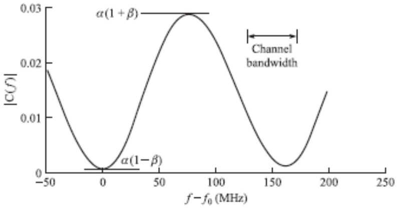

FIGURE 13.1–9
Magnitude frequency response of LOS channel model.

Deep fading phenomenon: At $f = f_0$, the so-called **deep fading** occurs.

13.2 The effect of signal characteristics on the choice of a channel model

Usually, we prefer **slowly fading** and **frequency non-selectivity**.

So we wish to choose symbol time T and transmission bandwidth B such that

$$T < (\Delta t)_c \quad \text{and} \quad B < (\Delta f)_c$$

Hence, using $BT = 1$, we wish

$$\frac{T}{(\Delta t)_c}\frac{B}{(\Delta f)_c} = B_d T_m < 1.$$

The term $B_d T_m$ is an essential channel parameter and is called **spread factor**.

Underspread versus overspread

Underspread $\equiv B_d T_m < 1$

Overspread $\equiv B_d T_m > 1$

MULTIPATH SPREAD, DOPPLER SPREAD, AND SPREAD FACTOR FOR SEVERAL TIME-VARIANT MULTIPATH CHANNELS

Type of channel	Multipath duration (sec)	Doppler spread (Hz)	Spread factor
Shortwave ionospheric propagation (HF)	10^{-3}–10^{-2}	10^{-1}–1	10^{-4}–10^{-2}
Ionospheric propagation under disturbed auroral conditions (HF)	10^{-3}–10^{-2}	10–100	10^{-2}–1
Ionospheric forward scatter (VHF)	10^{-4}	10	10^{-3}
Tropospheric scatter (SHF)	10^{-6}	10	10^{-5}
Orbital scatter (X band)	10^{-4}	10^{3}	10^{-1}
Moon at max. libration	10^{-2}	10	10^{-1}

13.3 Frequency-nonslective, slowly fading channel

For a frequency-nonslective, slowly fading channel, i.e.,

$$T_m \ll \frac{1}{B} = T \ll (\Delta t)_c,$$

the signal spectrum $s_\ell(f)$ is almost unchanged by $\mathbf{C}_\ell(f;t)$; hence,

$$\mathbf{C}_\ell(f;t) \approx \mathbf{C}_\ell(0;t) \text{ within the signal bandwidth}$$

and it is almost time-invariant; hence,

$$\mathbf{C}_\ell(f;t) \approx \mathbf{C}_\ell(0) \text{ within the signal bandwidth}$$

This gives

$$\begin{aligned} r_\ell(t) &= c_\ell(\tau;t) \star s_\ell(t) + z(t) \\ &= \int_{-\infty}^{\infty} \mathbf{C}_\ell(f;t) s_\ell(f) e^{-\imath 2\pi f t} df + z(t) \\ &\approx \int_{-\infty}^{\infty} \mathbf{C}_\ell(0) s_\ell(f) e^{-\imath 2\pi f t} df + z(t) = \mathbf{C}_\ell(0) s_\ell(t) + z(t) \end{aligned}$$

Assume that the phase of $\mathbf{C}_\ell(0) = \alpha e^{\imath\phi}$ can be perfectly estimated and compensated by the receiver. The channel model becomes:

$$r_\ell(t) = \alpha s_\ell(t) + z(t).$$

After demodulation (i.e., vectorization), we obtain

$$\boldsymbol{r}_\ell = \alpha \boldsymbol{s}_\ell + \boldsymbol{n}_\ell.$$

Question: What will the error probability be under random α?

Case 1: Equal-prior BPSK

$$r = \pm\alpha\sqrt{\mathcal{E}} + n \quad \text{(passband vectorization with } E[n^2] = \tfrac{N_0}{2}\text{)}$$
$$r_{\ell,\text{real}} = \pm\alpha\sqrt{2\mathcal{E}} + n_{\ell,\text{real}} \quad \text{(baseband vectorization with } E[n_{\ell,\text{real}}^2] = N_0\text{)}$$

The optimal decision is $r \lessgtr 0$, regardless of α (due to equal prior probability).

Thus,

$$\Pr\{\text{error}|\alpha\} = Q\left(\sqrt{2\alpha^2\frac{\mathcal{E}}{N_0}}\right)$$

Given that α is Rayleigh distributed (cf. Slide 4-167), we have

$$P_{e,BPSK} = \int_0^\infty \Pr\{\text{error}|\alpha\} \underbrace{\frac{\alpha}{\sigma^2}e^{-\frac{\alpha^2}{2\sigma^2}}}_{\text{Rayleigh}} d\alpha$$

where $\mathbb{E}[\alpha^2] = 2\sigma^2$.

$$
\begin{aligned}
P_{e,BPSK} &= \int_0^\infty Q\left(\beta\frac{\alpha}{\sigma}\right)\frac{\alpha}{\sigma^2}e^{-\frac{\alpha^2}{2\sigma^2}}d\alpha, \text{ where } \beta^2 = 2\sigma^2\frac{\mathcal{E}}{N_0} \\
&= \int_0^\infty Q(\beta x)xe^{-\frac{x^2}{2}}dx, \text{ where } x = \frac{\alpha}{\sigma} \\
&= Q(\beta x)\left(-e^{-\frac{x^2}{2}}\right)\Big|_0^\infty - \int_0^\infty\left(-\frac{\beta}{\sqrt{2\pi}}e^{-\frac{\beta^2x^2}{2}}\right)\left(-e^{-\frac{x^2}{2}}\right)dx \\
&= \frac{1}{2} - \sqrt{\frac{\beta^2}{1+\beta^2}}\int_0^\infty \frac{1}{\sqrt{2\pi\left(\frac{1}{1+\beta^2}\right)}}e^{-\frac{x^2}{2\left(\frac{1}{1+\beta^2}\right)}}dx \\
&= \frac{1}{2} - \frac{1}{2}\sqrt{\frac{\beta^2}{1+\beta^2}} \\
&= \frac{1}{2} - \frac{1}{2}\sqrt{\frac{\bar{\gamma}_b}{1+\bar{\gamma}_b}}, \text{ where } \bar{\gamma}_b = \mathbb{E}[\alpha^2]\frac{\mathcal{E}}{N_0} = (2\sigma^2)\left(\frac{\beta^2}{2\sigma^2}\right) = \beta^2
\end{aligned}
$$

$$
\left(= \frac{1}{2(1+\bar{\gamma}_b+\sqrt{\bar{\gamma}_b^2+\bar{\gamma}_b})} \approx \frac{1}{4\bar{\gamma}_b} \text{ when } \bar{\gamma}_b \text{ large}\right)
$$

Similarly, for BFSK,

$$\boldsymbol{r} = \left\{ \begin{bmatrix} \alpha\sqrt{\mathcal{E}} \\ 0 \end{bmatrix} \text{ or } \begin{bmatrix} 0 \\ \alpha\sqrt{\mathcal{E}} \end{bmatrix} \right\} + \boldsymbol{n}$$

Under equal prior, the optimal decision is $r_1 \lessgtr r_2$, regardless of α.

$$\begin{aligned}
P_{e,BFSK} &= \int_0^\infty \Pr\{\text{error}|\alpha\} f(\alpha) d\alpha \\
&= \int_0^\infty Q\left(\beta \frac{\alpha}{\sigma}\right) \frac{\alpha}{\sigma^2} e^{-\frac{\alpha^2}{2\sigma^2}} d\alpha, \text{ where now } \beta^2 = \sigma^2 \frac{\mathcal{E}}{N_0} \\
&= {\color{red}\frac{1}{2}} - {\color{blue}\frac{1}{2}\sqrt{\frac{\beta^2}{1+\beta^2}}} \\
&= {\color{red}\frac{1}{2}} - {\color{blue}\frac{1}{2}\sqrt{\frac{\bar{\gamma}_b}{2+\bar{\gamma}_b}}}, \text{ where } \bar{\gamma}_b = \mathbb{E}[\alpha^2]\frac{\mathcal{E}}{N_0} = 2\sigma^2\frac{\beta^2}{\sigma^2} = 2\beta^2 \\
\Bigg(&= \frac{1}{2 + \bar{\gamma}_b + \sqrt{\bar{\gamma}_b^2 + 2\bar{\gamma}_b}} \approx \frac{1}{2\bar{\gamma}_b} \text{ when } \bar{\gamma}_b \text{ large}\Bigg)
\end{aligned}$$

Case 3: BDPSK

$$
\begin{aligned}
P_{e,BDPSK} &= \int_0^\infty \Pr\{\text{error}|\alpha\} f(\alpha) d\alpha \\
&= \int_0^\infty \left(\frac{1}{2} e^{-\beta^2 \frac{\alpha^2}{2\sigma^2}}\right)\left(\frac{\alpha}{\sigma^2} e^{-\frac{\alpha^2}{2\sigma^2}}\right) d\alpha, \text{ where } \beta^2 = 2\sigma^2 \frac{\mathcal{E}}{N_0} \\
&= \frac{1}{2(1+\beta^2)} \int_0^\infty (1+\beta^2) x e^{-\left(\frac{1+\beta^2}{2}\right)x^2} dx \\
&= -\frac{1}{2(1+\beta^2)} e^{-\left(\frac{1+\beta^2}{2}\right)x^2}\Big|_0^\infty \\
&= \frac{1}{2(1+\bar{\gamma}_b)}, \text{ where } \bar{\gamma}_b = \mathbb{E}[\alpha^2]\frac{\mathcal{E}}{N_0} = 2\sigma^2 \frac{\beta^2}{2\sigma^2} = \beta^2 \\
&\approx \frac{1}{2\bar{\gamma}_b} \text{ when } \bar{\gamma}_b \text{ large}
\end{aligned}
$$

Case 4: Noncoherent BFSK

$$
\begin{aligned}
P_{e,noncoherent\ \ BFSK} &= \int_0^\infty \Pr\{\text{error}|\alpha\} f(\alpha) d\alpha \\
&= \int_0^\infty \left(\frac{1}{2} e^{-\beta^2 \frac{\alpha^2}{2\sigma^2}}\right)\left(\frac{\alpha}{\sigma^2} e^{-\frac{\alpha^2}{2\sigma^2}}\right) d\alpha, \text{ where } \beta^2 = \sigma^2 \frac{\mathcal{E}}{N_0} \\
&= \frac{1}{2(1+\beta^2)} \\
&= \frac{1}{2+\bar{\gamma}_b}, \text{ where } \bar{\gamma}_b = \mathbb{E}[\alpha^2] \frac{\mathcal{E}}{N_0} = 2\sigma^2 \frac{\beta^2}{\sigma^2} = 2\beta^2 \\
&\approx \frac{1}{\bar{\gamma}_b} \text{ when } \bar{\gamma}_b \text{ large}
\end{aligned}
$$

	P_e under AWGN	P_e under Rayleigh fading	Approx P_e under Rayleigh fading
BPSK	$Q(\sqrt{2\gamma_b})$	$\frac{1}{2}\left(1-\sqrt{\frac{\bar{\gamma}_b}{1+\bar{\gamma}_b}}\right)$	$\frac{1}{4\bar{\gamma}_b}$
BFSK	$Q(\sqrt{\gamma_b})$	$\frac{1}{2}\left(1-\sqrt{\frac{\bar{\gamma}_b}{2+\bar{\gamma}_b}}\right)$	$\frac{1}{2\bar{\gamma}_b}$
BDPSK	$\frac{1}{2}e^{-\gamma_b}$	$\frac{1}{2(1+\bar{\gamma}_b)}$	$\frac{1}{2\bar{\gamma}_b}$
Noncohrent BFSK	$\frac{1}{2}e^{-\gamma_b/2}$	$\frac{1}{2+\bar{\gamma}_b}$	$\frac{1}{\bar{\gamma}_b}$

- BPSK is 3dB better than BDPSK/BFSK; 6dB better than noncoherent BFSK.
- P_e decreases **inversely** proportional with SNR under fading.
- P_e decreases **exponentially** with SNR when **no** fading.

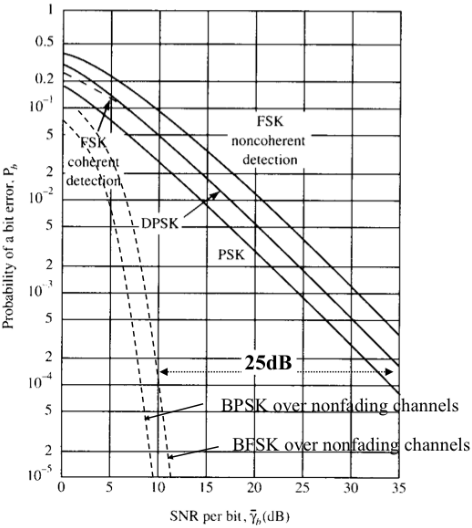

- To achieve $P_e = 10^{-4}$, the system must provide an SNR higher than 35dB, which is not practically possible!
- So an alternative solution should be used to compensate the fading such as the diversity technique.

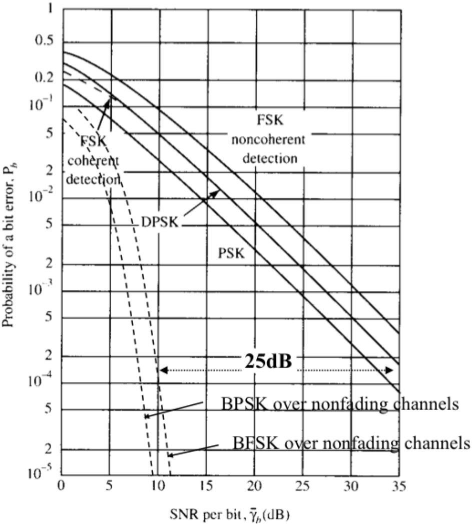

Nakagami fading

If $\alpha \equiv$ Nakagami-m fading,

Turin *et al.* (1972) and Suzuki (1977) have shown that the Nakagami-m distribution is the best-fit for urban radio multipath channels.

$\Longrightarrow \; f(\alpha) = \frac{2}{\Gamma(m)}\left(\frac{m}{\Omega}\right)^m \alpha^{2m-1} e^{-m\alpha^2/\Omega}$, where $\Omega = \mathbb{E}[\alpha^2]$.

- $m < 1$: Worse than Rayleigh fading in performance
- $m = 1$: Rayleigh fading
- $m > 1$: Better than Rayleigh fading in performance

Notably, $m = \frac{\mathbb{E}^2[\alpha^2]}{\mathrm{Var}[\alpha^2]} = \frac{\Omega^2}{\mathbb{E}[(\alpha^2-\Omega)^2]}$ is called the fading figure.

Prob density function of Nakagami-m with $\Omega = 1$

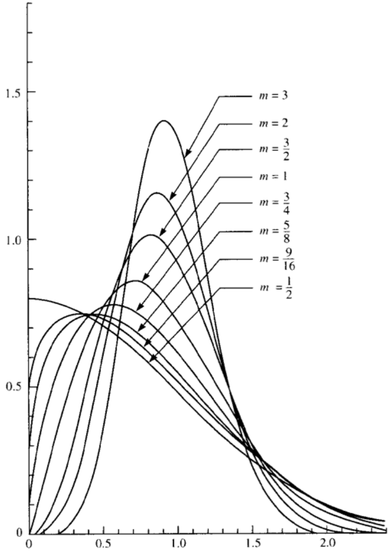

BPSK performance under Nakagami-m fading

$$P_{e,BPSK} = \int_0^\infty Q\left(\sqrt{2\alpha^2\mathcal{E}/N_0}\right) \underbrace{\frac{2}{\Gamma(m)}\left(\frac{m}{\Omega}\right)^m \alpha^{2m-1} e^{-m\alpha^2/\Omega}}_{f(\alpha)} d\alpha$$

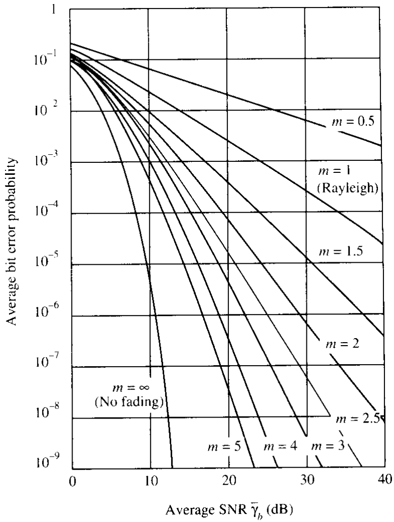

In some channel, the system performance may degrade even worse, such as Rummler's model in Slide 13-49, where **deep fading** occurs at some frequency.

$|\mathbf{C}_\ell(f)|$

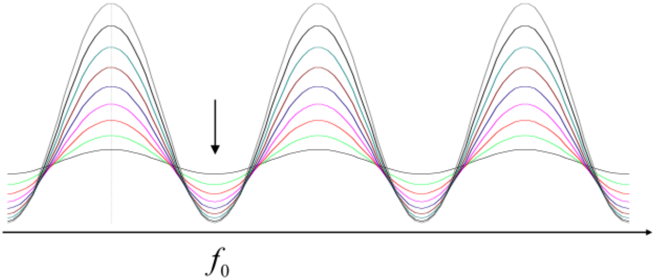

The lowest is equal to $\alpha(1-\beta)$, which is itself a random variable.

13.4 Diversity techniques for fading multipath channels

Solutions to compensate deep fading

- Frequency diversity
  - Separation of carriers $\geq (\Delta f)_c = 1/T_m$ to obtain uncorrelation in signal replicas.
- Time diversity
  - Separation of time slots $\geq (\Delta t)_c = 1/B_d$ to obtain uncorrelation in signal replicas.
- Space diversity (Multiple receiver antennas)
  - Spaced sufficiently far apart to ensure received signals faded independently (usually, $>$ 10 wavelengths)
- RAKE correlator or RAKE matched filter (Price and Green 1958)
  - It is named **wideband approach**, since it is usually applied to the situation where signal bandwidth is **much greater** than the coherent bandwidth $(\Delta f)_c$.

It is clear for the first three diversities, we will have L identical replicas at the Rx (which are uncorrelated).

The idea is that as long as not all of them are deep-faded, the demodulation is sufficiently good.

For the last one (i.e., RAKE), where $B \gg (\Delta f)_c$, which results in a frequency selective channel, we have

$$L = \frac{B}{(\Delta f)_c}.$$

Detail will be given in the following.

13.4-1 Binary signals

Assumption

1. *L identical and independent channels*
2. *Each channel is* **frequency-nonselective** *and* **slowly fading** *with Rayleigh-distributed envelope.*
3. *Zero-mean additive white Gaussian background noise*
4. *Assume the phase-shift can be perfectly compensated.*
5. *Assume the attenuation $\{\alpha_k\}_{k=1}^{L}$ can be perfectly estimated at Rx.*

Hence,

$$r_k = \alpha_k s + n_k \quad k = 1, 2, \ldots, L$$

How to combine these L outputs when making decision?
Maximal ratio combiner (Brennan 1959)

$$r = \sum_{k=1}^{L} \alpha_k r_k = \sum_{k=1}^{L} \alpha_k^2 s + \sum_{k=1}^{L} \alpha_k n_k$$

Idea behind maximal ratio combiner

- Trust more on the strong signals and trust less on the weak signal.

Advantage of maximal ratio combiner

- Theoretically tractable; so we can predict how "good" the system can achieve without performing simulations.
- Maximum-ratio combining is an optimum linear combiner.

Find $\{w_k\}_{k=1}^{L}$ for linear combiner

$$r = \sum_{k=1}^{L} w_k r_k = \sum_{k=1}^{L} w_k \alpha_k s + \sum_{k=1}^{L} w_k n_k$$

such that the output SNR

$$\left(\sum_{k=1}^{L} w_k \alpha_k\right)^2 \mathbb{E}[s^2] \Big/ \sum_{k=1}^{L} w_k^2 \mathbb{E}[n_k^2]$$

is maximized.

Case 1: Equal-prior BPSK

$$r = \pm\alpha\sqrt{\mathcal{E}} + n, \text{ where } \alpha = \sqrt{\sum_{k=1}^{L}\alpha_k^2} \text{ and } n = \frac{1}{\alpha}\sum_{k=1}^{L}\alpha_k n_k$$

The optimal decision is $r \lessgtr 0$, regardless of α.
Thus,

$$\Pr\{\text{error}|\alpha\} = Q\left(\sqrt{2\alpha^2\frac{\mathcal{E}}{N_0}}\right)$$

Given that $\{\alpha_k\}_{k=1}^{L}$ is i.i.d. Rayleigh distributed, α is Nakagami-L distributed; hence,

$$P_{e,BPSK} = \int_0^\infty \Pr\{\text{error}|\alpha\}\tfrac{2}{(L-1)!}\left(\tfrac{L}{\Omega}\right)^L\alpha^{2L-1}e^{-L\alpha^2/\Omega}d\alpha$$

where $\Omega = \mathbb{E}[\alpha^2] = L\cdot\mathbb{E}[\alpha_1^2] = 2L\sigma^2$.

Note $\{\alpha_k^2 = X_k^2 + Y_k^2\}_{k=1}^{L}$ is i.i.d. χ^2-distributed with 2 degree of freedom $\Rightarrow \alpha^2 = \sum_{k=1}^{L}\alpha_k^2 = X_1^2 + Y_1^2 + \cdots + X_L^2 + Y_L^2$ is χ^2-distributed with $2L$ degree of freedom, where $\{X_k\}_{k=1}^{L}$ and $\{Y_k\}_{k=1}^{L}$ zero-mean i.i.d. Gaussian.

$$
\begin{aligned}
P_{e,BPSK} &= \int_0^\infty Q(\beta\alpha)\,\tfrac{2}{(L-1)!}\left(\tfrac{1}{2\sigma^2}\right)^L \alpha^{2L-1} e^{-\alpha^2/(2\sigma^2)}\,d\alpha, \\
&\qquad \text{where } \beta = \sqrt{2\mathcal{E}/N_0} \\
&= \left(\frac{1-\mu}{2}\right)^L \cdot \sum_{k=0}^{L-1} \binom{L-1+k}{k} \left(\frac{1+\mu}{2}\right)^k \\
&\qquad \text{where } \mu = \sqrt{\tfrac{\bar{\gamma}_c}{1+\bar{\gamma}_c}} \text{ and } \bar{\gamma}_c = \mathbb{E}[\alpha_k^2]\tfrac{\mathcal{E}}{N_0} \\
&\left(\approx \binom{2L-1}{L}\left(\frac{1}{4\bar{\gamma}_c}\right)^L \text{ when } \bar{\gamma}_c \text{ large} \right)
\end{aligned}
$$

where we have $\frac{1-\mu}{2} = \frac{1}{2(1+\bar{\gamma}_c+\sqrt{\bar{\gamma}_c^2+\bar{\gamma}_c})} \approx \frac{1}{4\bar{\gamma}_c}$ and $\frac{1+\mu}{2} \approx 1$.

For your reference: $L = 2$

$$\begin{aligned}
P_{e,BPSK} &= \int_0^\infty Q\left(\beta\frac{\alpha}{\sigma}\right)2\left(\frac{1}{2\sigma^2}\right)^2\alpha^3 e^{-\frac{\alpha^2}{2\sigma^2}}d\alpha, \text{ where } \beta^2 = 2\sigma^2\frac{\mathcal{E}}{N_0}\\
&= \int_0^\infty Q(\beta x)\frac{1}{2}x^3 e^{-\frac{x^2}{2}}dx\\
&= Q(\beta x)\left(-\frac{(x^2+2)}{2}e^{-\frac{x^2}{2}}\right)\Bigg|_0^\infty - \int_0^\infty\left(-\frac{\beta}{\sqrt{2\pi}}e^{-\frac{\beta^2x^2}{2}}\right)\left(-\frac{(x^2+2)}{2}e^{-\frac{x^2}{2}}\right)dx\\
&= \frac{1}{2} - \int_0^\infty \frac{\beta}{2\sqrt{2\pi}}(x^2+2)e^{-\frac{(1+\beta^2)x^2}{2}}dx\\
&= \frac{1}{2} - \frac{1}{4}\sqrt{\frac{\beta^2}{1+\beta^2}}\int_{-\infty}^\infty (x^2+2)\frac{1}{\sqrt{2\pi\frac{1}{(1+\beta^2)}}}e^{-\frac{x^2}{2\frac{1}{(1+\beta^2)}}}dx\\
&= \frac{1}{2} - \frac{1}{4}\sqrt{\frac{\beta^2}{1+\beta^2}}\left[\frac{1}{(1+\beta^2)}+2\right]\\
&= \frac{1}{2} - \frac{1}{4}\mu((1-\mu^2)+2), \text{ where } \bar{\gamma}_c = \mathbb{E}[\alpha_k^2]\frac{\mathcal{E}}{N_0} = \beta^2 \text{ and } \mu = \sqrt{\frac{\bar{\gamma}_c}{1+\bar{\gamma}_c}}\\
&= \left(\frac{1-\mu}{2}\right)^2\cdot\left(1+2\left(\frac{1+\mu}{2}\right)^1\right)
\end{aligned}$$

Case 2: Equal-prior BFSK

Similarly, for BFSK,

$$\boldsymbol{r} = \left\{ \begin{bmatrix} \alpha\sqrt{\mathcal{E}} \\ 0 \end{bmatrix} \text{ or } \begin{bmatrix} 0 \\ \alpha\sqrt{\mathcal{E}} \end{bmatrix} \right\} + \boldsymbol{n}$$

The optimal decision is $r_1 \lessgtr r_2$, regardless of α.

$$\begin{aligned} P_{e,BFSK} &= \int_0^\infty Q(\beta\alpha) \tfrac{2}{(L-1)!} \left(\tfrac{1}{2\sigma^2}\right)^L \alpha^{2L-1} e^{-\alpha^2/(2\sigma^2)} d\alpha, \\ & \qquad \text{where } \beta^2 = \sigma^2 \tfrac{\mathcal{E}}{N_0} \\ &= \left(\frac{1-\mu}{2}\right)^L \cdot \sum_{k=0}^{L-1} \binom{L-1+k}{k} \left(\frac{1+\mu}{2}\right)^k \\ & \qquad \text{where } \mu = \sqrt{\tfrac{\bar{\gamma}_c}{2+\bar{\gamma}_c}} \text{ and } \bar{\gamma}_c = \mathbb{E}[\alpha_k^2] \tfrac{\mathcal{E}}{N_0} \\ \left(\approx \right. & \left. \left(\frac{1}{2\bar{\gamma}_c}\right)^L \binom{2L-1}{L} \text{ when } \bar{\gamma}_c \text{ large} \right) \end{aligned}$$

Case 3: BDPSK

From Slide 4-175, the two consecutive lowpass equivalent signals are

$$\boldsymbol{s}_\ell^{(k-1)} = \sqrt{2\mathcal{E}}e^{\imath\phi_0} \quad \text{and} \quad \boldsymbol{s}_\ell^{(k)} = \begin{cases} \sqrt{2\mathcal{E}}e^{\imath\phi_0}, & m = 1; \\ -\sqrt{2\mathcal{E}}e^{\imath\phi_0}, & m = 2 \end{cases}$$

The L received signals given $\boldsymbol{s}_\ell^{(k-1)}$ and $\boldsymbol{s}_\ell^{(k)}$ are

$$\vec{\boldsymbol{r}}_{j,\ell} = \begin{bmatrix} \boldsymbol{r}_{j,\ell}^{(k-1)} \\ \boldsymbol{r}_{j,\ell}^{(k)} \end{bmatrix} = \alpha_j e^{\imath\phi_j} \begin{bmatrix} \boldsymbol{s}_\ell^{(k-1)} \\ \boldsymbol{s}_\ell^{(k)} \end{bmatrix} + \begin{bmatrix} \boldsymbol{n}_{j,\ell}^{(k-1)} \\ \boldsymbol{n}_{j,\ell}^{(k)} \end{bmatrix} = \alpha_j e^{\imath\phi_j} \vec{\boldsymbol{s}}_\ell + \vec{\boldsymbol{n}}_{j,\ell}$$

for $j = 1, \ldots, L$.

Note that it is unnecessary to estimate α_j and ϕ_j for jth reception as required by Cases 1 & 2.

$$\Rightarrow \vec{\boldsymbol{s}}_{j,\ell}^\dagger \vec{\boldsymbol{r}}_{j,\ell} = \begin{bmatrix} \sqrt{2\mathcal{E}}e^{-\imath\phi_0} & \pm\sqrt{2\mathcal{E}}e^{-\imath\phi_0} \end{bmatrix} \begin{bmatrix} \boldsymbol{r}_{j,\ell}^{(k-1)} \\ \boldsymbol{r}_{j,\ell}^{(k)} \end{bmatrix}$$

$$= \begin{cases} \sqrt{2\mathcal{E}}e^{-\imath\phi_0}\left(\boldsymbol{r}_{j,\ell}^{(k-1)} + \boldsymbol{r}_{j,\ell}^{(k)}\right), & m = 1 \\ \sqrt{2\mathcal{E}}e^{-\imath\phi_0}\left(\boldsymbol{r}_{j,\ell}^{(k-1)} - \boldsymbol{r}_{j,\ell}^{(k)}\right), & m = 2 \end{cases}$$

Instead of **maximal ratio combining**, we do **square-law combining**:

$$\begin{aligned}
\hat{m} &= \arg\max_{1\le m\le 2} \sum_{j=1}^{L} \left|\vec{\boldsymbol{s}}_{j,\ell}^{\dagger} \vec{\boldsymbol{r}_{j,\ell}}\right|^2 \\
&= \arg\max \left\{ \underbrace{\sum_{j=1}^{L} \left|\boldsymbol{r}_{j,\ell}^{(k-1)} + \boldsymbol{r}_{j,\ell}^{(k)}\right|^2}_{m=1}, \underbrace{\sum_{j=1}^{L} \left|\boldsymbol{r}_{j,\ell}^{(k-1)} - \boldsymbol{r}_{j,\ell}^{(k)}\right|^2}_{m=2} \right\} \\
&= \arg\max \left\{ \underbrace{U_\ell}_{m=1}, \underbrace{-U_\ell}_{m=2} \right\}
\end{aligned}$$

where $U_\ell = \sum_{j=1}^{L} \mathbf{Re}\left\{\left(\boldsymbol{r}_{j,\ell}^{(k-1)}\right)^* \boldsymbol{r}_{j,\ell}^{(k)}\right\}$.

The quadratic-form analysis (cf. Slide 4-176) gives

$$P_{e,BDPSK} = \left(\frac{1-\mu}{2}\right)^L \cdot \sum_{k=0}^{L-1} \binom{L-1+k}{k} \left(\frac{1+\mu}{2}\right)^k$$

$$\textbf{with } \mu = \frac{\bar{\gamma}_c}{1+\bar{\gamma}_c}$$

$$\approx \left(\frac{1}{2\bar{\gamma}_c}\right)^L \binom{2L-1}{L} \text{ when } \bar{\gamma}_c \text{ large.}$$

Case 4: Noncoherent BFSK

Recall from Slide 4-165:

The noncoherent ML computes

$$\hat{m} = \arg\max_{1\le m\le 2} \left| \boldsymbol{r}_\ell^\dagger \boldsymbol{s}_{m,\ell} \right|$$

$$\begin{array}{rl} \boldsymbol{s}_{1,\ell} = & \begin{pmatrix} \sqrt{2\mathcal{E}_s} & 0 \end{pmatrix} \\ \boldsymbol{s}_{2,\ell} = & \begin{pmatrix} 0 & \sqrt{2\mathcal{E}_s} \end{pmatrix} \end{array}$$

Hence,

$$\hat{m} = \arg\max_{1\le m\le 2} \left| r_{m,\ell} \right| = \arg\max_{1\le m\le 2} \left| r_{m,\ell} \right|^2$$

Now we have L diversities/channels:

$$\boldsymbol{r}_{j,\ell} = \begin{bmatrix} r_{j,1,\ell} \\ r_{j,2,\ell} \end{bmatrix} = \alpha_j e^{\imath \phi_j} \boldsymbol{s}_{m,\ell} + \boldsymbol{n}_{j,\ell} \quad j = 1, 2, \ldots, L$$

Instead of **maximal ratio combining**, we again do **square-law combining**:

$$\hat{m} = \arg \max_{1 \le m \le 2} \sum_{j=1}^{L} \left| \boldsymbol{r}_{j,m,\ell} \right|^2 .$$

$$\begin{aligned} P_{e,noncoherent\ \ BFSK} &= \left(\frac{1-\mu}{2}\right)^L \cdot \sum_{k=0}^{L-1} \binom{L-1+k}{k} \left(\frac{1+\mu}{2}\right)^k \\ &\qquad \textbf{with } \mu = \frac{\bar{\gamma}_c}{2+\bar{\gamma}_c} \\ &\approx \left(\frac{1}{\bar{\gamma}_c}\right)^L \binom{2L-1}{L} \text{ when } \bar{\gamma}_c \text{ large.} \end{aligned}$$

Summary (what the theoretical results indicate?)

- With Lth order diversity, the POE decreases inversely with Lth power of the SNR.

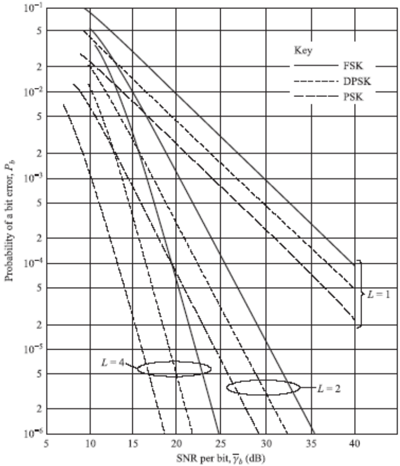

FIGURE 13.4–2
Performance of binary signals with diversity.

In Cases 1 & 2, comparing the prob density functions of α for 1-diversity (no diversity) **Nakagami fading** and L-diversity **Rayleigh fading**, we conclude:

L-diversity in Rayleigh fading = 1-diversity in Nakagami-L

or further

mL-diversity in Rayleigh fading = L-diversity in Nakagami-m

13.4-2 Multiphase signals

For M-ary phase signal over L Rayleigh fading channels, the symbol error rate P_e can be derived as (Appendix C)

$$\begin{aligned} P_e &= \frac{(-1)^{L-1}(1-\mu^2)^L}{\pi(L-1)!}\left(\frac{\partial^{L-1}}{\partial b^{L-1}}\left\{\frac{1}{b-\mu^2}\left[\frac{\pi}{M}(M-1)\right.\right.\right. \\ &\qquad \left.\left.\left.-\frac{\mu\sin(\pi/M)}{\sqrt{b-\mu^2\cos^2(\pi/M)}}\cot^{-1}\left(\frac{-\mu\cos(\pi/M)}{\sqrt{b-\mu^2\cos^2(\pi/M)}}\right)\right]\right\}\right)\Bigg|_{b=1} \\ &\approx \begin{cases} \frac{M-1}{\log_2(M)\sin^2(\pi/M)}\frac{1}{2M\gamma_b} & M\text{-ary PSK \& L=1} \\ \frac{M-1}{\log_2(M)\sin^2(\pi/M)}\frac{1}{M\gamma_b} & M\text{-ary DPSK \& L=1} \end{cases} \end{aligned}$$

where

$$\mu = \begin{cases} \sqrt{\frac{\bar{\gamma}_c}{1+\bar{\gamma}_c}} & M\text{-ary PSK} \\ \frac{\bar{\gamma}_c}{1+\bar{\gamma}_c} & M\text{-ary DPSK} \end{cases}$$

and in this case, the system SNR $\bar{\gamma}_t = \bar{\gamma}_b \log_2(M) = L\bar{\gamma}_c$.

PSK is about 3dB better than DPSK for all M ($L = 1$).

Recall Slide 4-180 under AWGN,
BDPSK is 1 dB inferior than BPSK
and
QDPSK is 2.3 dB inferior than QPSK.

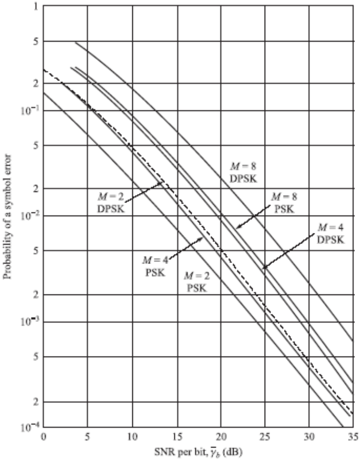

FIGURE 13.4–3
Probability of symbol error for PSK and DPSK for Rayleigh fading.

DPSK performance with diversity

- Bit error P_b is calculated based on Gray coding.
- Larger M, worse P_b except for equal P_b at $M = 2, 4$.

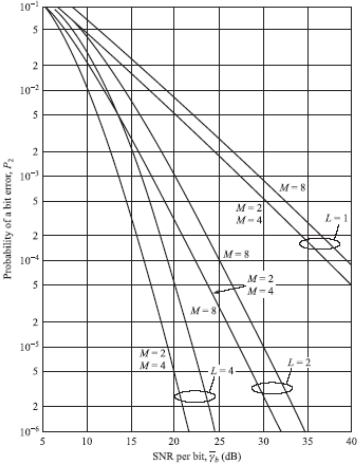

FIGURE 13.4–4
Probability of a bit error for DPSK with diversity for Rayleigh fading.

13.4-3 M-ary orthogonal signals

Noncoherent detection

- Here, the derivation assumes that both passband and lowpass equivalent signals are orthogonal; hence, the frequency separation is $1/T$ rather than $1/(2T)$.
- Based on lowpass (baseband) orthogonality, L-diversity square-law combining gives

$$\begin{aligned} P_e &= \frac{1}{(L-1)!}\sum_{m=1}^{M-1}\frac{(-1)^{m+1}\binom{M-1}{m}}{(1+m+m\bar{\gamma}_c)^L} \\ &\quad \sum_{k=0}^{m(L-1)}\beta_{k,m}(L-1+k)!\left(\frac{1+\bar{\gamma}_c}{1+m+m\bar{\gamma}_c}\right)^k \end{aligned}$$

where $\beta_{k,m}$ is the coefficient of U^k in $\left(\sum_{k=0}^{L-1}\frac{U^k}{k!}\right)^m$, i.e.,

$$\left(\sum_{k=0}^{L-1}\frac{U^k}{k!}\right)^m = \sum_{k=0}^{m(L-1)}\beta_{k,m}U^k.$$

$M = 2$ **case:**

- Let $\bar{\gamma}_t = L\bar{\gamma}_c$ be the total system power.
For fixed $\bar{\gamma}_t$, there is an L that minimizes P_e.
- This hints that

$$\bar{\gamma}_c = 3 \approx 4.77 \text{ dB}$$

gives the best performance.

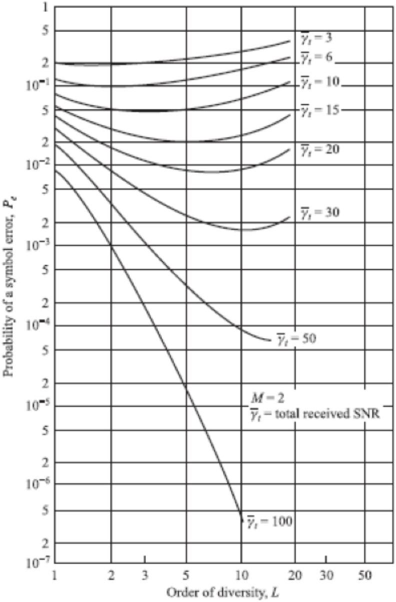

$M = 4$ **case:**

- Let $\bar{\gamma}_t = L\bar{\gamma}_c$ be the total system power.
  For fixed $\bar{\gamma}_t$, there is an L that minimizes P_e.
- This hints that

$$\bar{\gamma}_c = 3 \approx 4.77 \text{ dB}$$

gives the best performance.

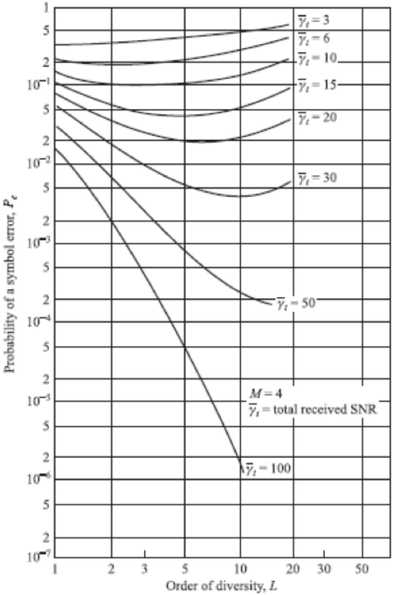

Discussions:

- Larger M, better performance but larger bandwidth.
- Larger L, better performance.
- An increase in L is more efficient in performance gain than an increase in M.

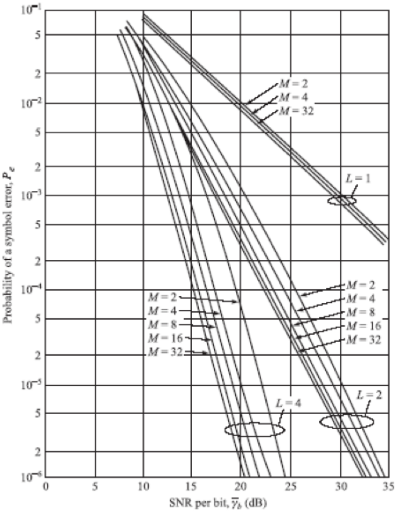

13.5 Digital signaling over a frequency-selective, slowly fading channel

13.5.1 A tapped-delay-line channel model

Assumption (Time-invariant channel)

$$c_\ell(\tau; t) = c_\ell(\tau)$$

Assumption (Bandlimited signal)

$s_\ell(t)$ *is band-limited, i.e.,* $|s_\ell(f)| = 0$ *for* $|f| > W/2$

In such case, we shall add a lowpass filter at the Rx.

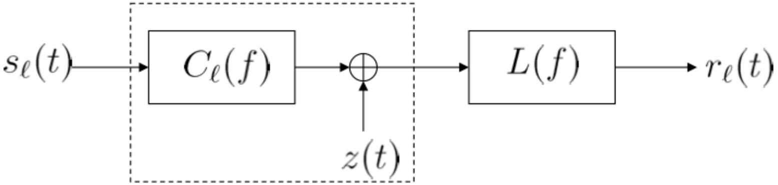

where $L(f) = \begin{cases} 1, & |f| \le W/2 \\ 0 & \text{otherwise} \end{cases}.$

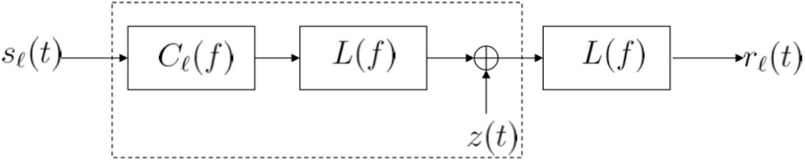

Equivalent channel with $C_\ell(f)$ random

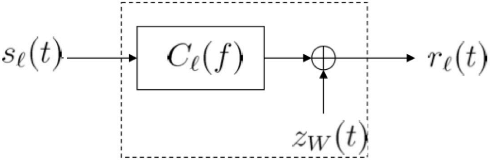

Equivalent channel with $C_\ell(f)$ random and bandlimited, and $z_W(t)$ bandlimited white noise

$$r_\ell(t) = \int_{-\infty}^{\infty} s_\ell(f)\mathbf{C}_\ell(f)e^{\imath 2\pi ft}df + z_W(t)$$

For a bandlimited $\mathbf{C}_\ell(f)$, sampling theorem gives:

$$\begin{cases} c_\ell(t) = \displaystyle\sum_{n=-\infty}^{\infty} c_\ell\left(\frac{n}{W}\right) \text{sinc}\left(W\left(t - \frac{n}{W}\right)\right) \\ \mathbf{C}_\ell(f) = \displaystyle\int_{-\infty}^{\infty} c_\ell(t) e^{-\imath 2\pi f t} dt \\ \qquad = \begin{cases} \dfrac{1}{W} \displaystyle\sum_{n=-\infty}^{\infty} c_\ell\left(\frac{n}{W}\right) e^{-\imath 2\pi f n/W}, & |f| \leq W/2 \\ 0, & \text{otherwise} \end{cases} \end{cases}$$

$$
\begin{aligned}
r_\ell(t) &= \int_{-\infty}^{\infty} s_\ell(f)\mathbf{C}_\ell(f)e^{\imath 2\pi ft}df + z_W(t) \\
&= \frac{1}{W}\sum_{n=-\infty}^{\infty} c_\ell\left(\frac{n}{W}\right)\int_{-W/2}^{W/2} s_\ell(f)e^{\imath 2\pi f(t-n/W)}df + z_W(t) \\
&= \frac{1}{W}\sum_{n=-\infty}^{\infty} c_\ell\left(\frac{n}{W}\right)s_\ell\left(t-\frac{n}{W}\right) + z_W(t) \\
&= \sum_{n=-\infty}^{\infty} c_n \cdot s_\ell\left(t-\frac{n}{W}\right) + z_W(t), \text{ where } c_n = \frac{1}{W}c_\ell\left(\frac{n}{W}\right)
\end{aligned}
$$

For a time-varying channel, we replace $c_\ell(\tau)$ and $\mathbf{C}_\ell(f)$ by $c_\ell(\tau; t)$ and $\mathbf{C}_\ell(f; t)$ and obtain

$$
r_\ell(t) = \sum_{n=-\infty}^{\infty} c_n(t) \cdot s_\ell\left(t-\frac{n}{W}\right) + z_W(t)
$$

where $c_n(t) = \frac{1}{W}c_\ell\left(\frac{n}{W}; t\right)$.

Statistically, with probability one, $c_\ell(\tau) = 0$ for $\tau > T_m$ and $\tau < 0$.

So, $c_\ell(\tau)$ is assumed band-limited and is also statistically time-limited!

Hence, $c_n(t) = 0$ for $n < 0$ and $n > T_m W$ (since $\tau = n/W > T_m$).

$$r_\ell(t) = \sum_{n=0}^{\lfloor T_m W \rfloor} c_n(t) \cdot s_\ell\left(t - \frac{n}{W}\right) + z_W(t)$$

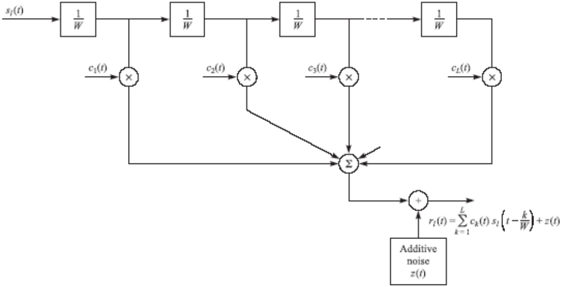

FIGURE 13.5–1
Trapped delay line model of frequency-selective channel.

For convenience, the text re-indexes the system as

$$r_\ell(t) = \sum_{k=1}^{L} c_k(t) \cdot s_\ell\left(t - \frac{k}{W}\right) + z_W(t).$$

13.5-2 The RAKE demodulator

Assumption (Gaussian and US (uncorrelated scattering))

$\{c_k(t)\}_{k=1}^{L}$ *complex i.i.d. Gaussian and can be perfectly estimated by Rx.*

So the Rx can regard the "transmitted signal" as one of

$$\begin{cases} v_{1,\ell}(t) = \sum_{k=1}^{L} c_k(t) \cdot s_{1,\ell}\left(t - \frac{k}{W}\right) \\ \vdots \\ v_{M,\ell}(t) = \sum_{k=1}^{L} c_k(t) \cdot s_{M,\ell}\left(t - \frac{k}{W}\right) \end{cases}$$

So Slide 4-158 said:

Coherent MAP detection

$$\begin{aligned} \hat{m} &= \arg\max_{1\le m\le M} \mathbf{Re}\left[\boldsymbol{r}_\ell^\dagger v_{m,\ell}\right] = \arg\max_{1\le m\le M} \mathbf{Re}\left[\int_0^T r_\ell(t) v_{m,\ell}^*(t)\,dt\right] \\ &= \arg\max_{1\le m\le M} \underbrace{\mathbf{Re}\left[\sum_{k=1}^{L}\int_0^T r_\ell(t) c_k^*(t) s_{m,\ell}^*\left(t-\frac{k}{W}\right)dt\right]}_{U_{m,\ell}} \end{aligned}$$

Discussions on assumptions: We assume:

- $s_\ell(t)$ is band-limited to W.
- $c_\ell(\tau)$ is causal and (statistically) time-limited to T_m and, at the same time, band-limited to W.
- $W \gg (\Delta f)_c = \frac{1}{T_m}$ (i.e., $L \approx WT_m \gg 1$)
- The definition of $U_{m,\ell}$ requires $T \gg T_m$ (See page 871 in textbook) such that the longest delayed version

$$s_\ell(t - L/W) = s_\ell(t - WT_m/W) = s_\ell(t - T_m)$$

is still well-confined within the integration range $[0, T)$. As a result, the signal bandwidth is much larger than $1/T$; RAKE is used in the demodulation of "spread-spectrum" signals!

$$WT \gg L \approx WT_m \gg 1 \implies W \gg \frac{1}{T}$$

$M = 2$ case

The receiver **collects** the signal energy from all received paths, which is somewhat analogous to the **garden rake** that is used to gather leaves, hays, etc. Consequently, the name "RAKE receiver" has been coined for this receiver structure by Price and Green (1958). (I use $s_{m,\ell}$, but the text uses $s_{\ell,m}$.)

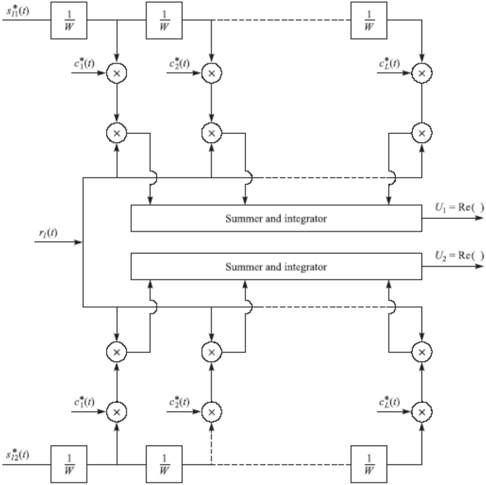

FIGURE 13.5–2
Optimum demodulator for wideband binary signals (delayed reference configuration).

An alternative realization of RAKE receiver

The previous structure requires M delay lines.

We can reduce the number of the delay lines to **one** by the following derivation.

Let $u = t - \frac{k}{W}$.

$$\begin{aligned}
U_{m,\ell} &= \mathbf{Re}\left[\sum_{k=1}^{L}\int_0^T r_\ell(t)c_k^*(t)s_{m,\ell}^*\left(t-\frac{k}{W}\right)dt\right] \\
&= \mathbf{Re}\left[\sum_{k=1}^{L}\int_{-k/W}^{T-k/W} r_\ell\left(u+\frac{k}{W}\right)c_k^*\left(u+\frac{k}{W}\right)s_{m,\ell}^*(u)\,du\right] \\
&\approx \mathbf{Re}\left[\sum_{k=1}^{L}\int_0^T r_\ell\left(t+\frac{k}{W}\right)c_k^*\left(t+\frac{k}{W}\right)s_{m,\ell}^*(t)\,dt\right]
\end{aligned}$$

where the last approximation follows from
$\left|\frac{k}{W}\right| \le \left|\frac{L}{W}\right| \approx \left|\frac{T_m W}{W}\right| = T_m \ll T$ (See Slide 13-104).

$r_\ell\left(t+\frac{L}{W}\right)$ $r_\ell\left(t+\frac{L-1}{W}\right)$ $\cdots$ $r_\ell\left(t+\frac{1}{W}\right)$

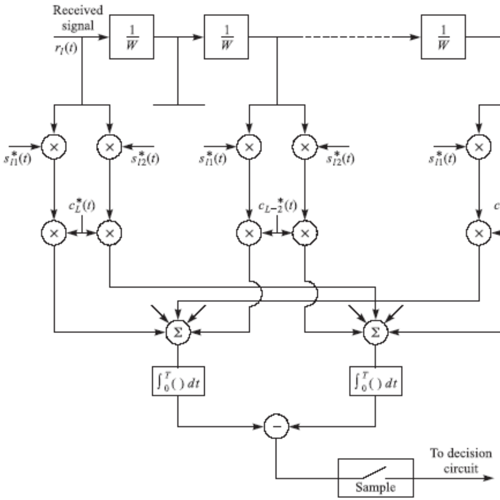

FIGURE 13.5–3
Optimum demodulator for wideband binary signals (delayed received signal configuration).

$c_k^*\left(t+\frac{k}{W}\right)=\frac{1}{W}c_\ell^*\left(\frac{k}{W};t+\frac{k}{W}\right)$ is abbreviated as $c_k^*(t)$ in the above figure.

Suppose $c_k(t) = c_k$ and the signal corresponding to $m = 1$ is transmitted. Then, letting $\tilde{U}_{m,\ell} = \frac{1}{\sqrt{2\mathcal{E}_s}} U_{m,\ell}$ and $\tilde{s}^*_{m,\ell}\left(t - \frac{k}{W}\right) = \frac{1}{\sqrt{2\mathcal{E}_s}} s^*_{m,\ell}\left(t - \frac{k}{W}\right)$ (normalization), we have

$$
\begin{aligned}
\tilde{U}_{m,\ell} &= \mathbf{Re}\left[\sum_{k=1}^{L}\int_0^T r_\ell(t) c_k^* \tilde{s}^*_{m,\ell}\left(t - \frac{k}{W}\right) dt\right] \\
&= \mathbf{Re}\left[\sum_{k=1}^{L}\int_0^T \underbrace{\left(\sum_{n=1}^{L} c_n s_{1,\ell}\left(t - \frac{n}{W}\right) + z_W(t)\right)}_{m=1} c_k^* \tilde{s}^*_{m,\ell}\left(t - \frac{k}{W}\right) dt\right] \\
&= \mathbf{Re}\left[\sum_{k=1}^{L}\sum_{n=1}^{L} c_n c_k^* \int_0^T s_{1,\ell}\left(t - \frac{n}{W}\right) \tilde{s}^*_{m,\ell}\left(t - \frac{k}{W}\right) dt\right] \\
&\quad + \mathbf{Re}\left[\sum_{k=1}^{L} c_k^* \int_0^T z_W(t) \tilde{s}^*_{m,\ell}\left(t - \frac{k}{W}\right) dt\right]
\end{aligned}
$$

Assumption (Add-and-delay property)

The transmitted signal is orthogonal to the shifted counterparts of all signals, including itself.

- $\left\{z_k = \int_0^T z_W(t)\tilde{s}^*_{m,\ell}\left(t - \frac{k}{W}\right)dt\right\}_{k=1}^L$ complex Gaussian with $E[|z_k|^2] = 2N_0$ because $\{\tilde{s}^*_{m,\ell}\left(t - \frac{k}{W}\right)\}_{k=1}^L$ orthonormal.

Hence, with $\alpha_k = |c_k|$,

$$\begin{aligned}\tilde{U}_{m,\ell} &= \mathbf{Re}\left[\sum_{k=1}^L |c_k|^2 \int_0^T s_{1,\ell}\left(t - \frac{k}{W}\right)\tilde{s}^*_{m,\ell}\left(t - \frac{k}{W}\right)dt\right] + \mathbf{Re}\left[\sum_{k=1}^L c_k^* z_k\right] \\ &= \sum_{k=1}^L \alpha_k^2 \mathbf{Re}\left[\left\langle s_{1,\ell}\left(t - \frac{k}{W}\right), \tilde{s}_{m,\ell}\left(t - \frac{k}{W}\right)\right\rangle\right] + \sum_{k=1}^L \alpha_k n_{k,\ell},\end{aligned}$$

where $\{n_{k,\ell} = \mathbf{Re}[e^{-\imath \angle c_k} z_k]\}_{k=1}^L$ i.i.d. Gaussian with $E[n_{k,\ell}^2] = N_0$.

- Under $T \gg T_m$, $\int_0^T s_{1,\ell}\left(t - \frac{k}{W}\right)\tilde{s}^*_{m,\ell}\left(t - \frac{k}{W}\right)dt$ is almost functionally independent of k; so,

$$\left\langle s_{1,\ell}\left(t - \tfrac{k}{W}\right), \tilde{s}_{m,\ell}\left(t - \tfrac{k}{W}\right)\right\rangle \approx \left\langle s_{1,\ell}(t), \tilde{s}_{m,\ell}(t)\right\rangle.$$

Therefore, the performance of RAKE is the same as the L-diversity maximal ratio combiner if $\{\alpha_k\}_{k=1}^L$ i.i.d.
However, $\{\alpha_k = |c_k|\}_{k=1}^L$ may not be identically distributed.

In such case, we can still obtain the pdf of $\gamma_b = \sum_{k=1}^L \gamma_k = \sum_{k=1}^L \alpha_k^2 \mathcal{E}_s/N_0 = \alpha^2 \mathcal{E}_s/N_0$ from

$$\begin{cases} \text{characteristic function of } \gamma_k \equiv \Psi_k(\imath\nu) = \dfrac{1}{1 - \imath\nu\bar{\gamma}_k} \\ \text{characteristic function of } \gamma_b = \displaystyle\sum_{k=1}^L \gamma_k \equiv \prod_{k=1}^L \Psi_k(\imath\nu) = \prod_{k=1}^L \frac{1}{1 - \imath\nu\bar{\gamma}_k} \end{cases}$$

The pdf of γ_b is then given by the Fourier transform of characteristic function:

$$f(\gamma_b) = \sum_{k=1}^L \frac{\pi_k}{\bar{\gamma}_k} e^{-\gamma_b/\bar{\gamma}_k}$$

where with $\bar{\gamma}_k = \mathbb{E}[\gamma_k]$, $\pi_k = \displaystyle\prod_{i=1, i\neq k}^L \frac{\bar{\gamma}_k}{\bar{\gamma}_k - \bar{\gamma}_i}$, provided $\bar{\gamma}_k \neq \bar{\gamma}_i$ for $k \neq i$.

$$\begin{cases} \text{BPSK}: \begin{cases} U_{1,\ell} \approx \sum_{k=1}^{L} \alpha_k^2 \mathbf{Re}\left[\left\langle s_{1,\ell}(t), \tilde{s}_{1,\ell}(t)\right\rangle\right] + \sum_{k=1}^{L} \alpha_k n_{k,\ell} \\ U_{2,\ell} \approx \sum_{k=1}^{L} \alpha_k^2 \mathbf{Re}\left[\left\langle s_{1,\ell}(t), \tilde{s}_{2,\ell}(t)\right\rangle\right] + \sum_{k=1}^{L} \alpha_k n_{k,\ell} \end{cases} \\ \text{BFSK}: \begin{cases} U_{1,\ell} \approx \sum_{k=1}^{L} \alpha_k^2 \mathbf{Re}\left[\left\langle s_{1,\ell}(t), \tilde{s}_{1,\ell}(t)\right\rangle\right] + \sum_{k=1}^{L} \alpha_k n_{k,\ell} \\ U_{2,\ell} \approx \sum_{k=1}^{L} \alpha_k^2 \mathbf{Re}\left[\left\langle s_{1,\ell}(t), \tilde{s}_{2,\ell}(t)\right\rangle\right] + \sum_{k=1}^{L} \alpha_k n_{k,\ell} \end{cases} \end{cases}$$

$$\Rightarrow \begin{cases} \text{BPSK}: \begin{cases} U_{1,\ell} \approx \sum_{k=1}^{L} \alpha_k^2 \sqrt{2\mathcal{E}_s} + \sum_{k=1}^{L} \alpha_k n_{k,\ell} \\ U_{2,\ell} \approx \sum_{k=1}^{L} \alpha_k^2 (-\sqrt{2\mathcal{E}_s}) + \sum_{k=1}^{L} \alpha_k n_{k,\ell} \end{cases} \\ \text{BFSK}: \begin{cases} U_{1,\ell} \approx \sum_{k=1}^{L} \alpha_k^2 \sqrt{2\mathcal{E}_s} + \sum_{k=1}^{L} \alpha_k n_{k,\ell} \\ U_{2,\ell} \approx \sum_{k=1}^{L} \alpha_k^2 \cdot (0) + \sum_{k=1}^{L} \alpha_k n_{k,\ell} \end{cases} \end{cases} \text{with } E[n_{k,\ell}^2] = N_0$$

Then,

$$P_e = \begin{cases} \frac{1}{2} \sum_{k=1}^{L} \pi_k \left(1 - \sqrt{\frac{\bar{\gamma}_k}{1+\bar{\gamma}_k}}\right) \approx \binom{2L-1}{L} \prod_{k=1}^{L} \frac{1}{4\bar{\gamma}_k}, & \text{BPSK, RAKE} \\ \frac{1}{2} \sum_{k=1}^{L} \pi_k \left(1 - \sqrt{\frac{\bar{\gamma}_k}{2+\bar{\gamma}_k}}\right) \approx \binom{2L-1}{L} \prod_{k=1}^{L} \frac{1}{2\bar{\gamma}_k}, & \text{BFSK, RAKE} \end{cases}$$

Estimation of c_k

For orthogonal signaling, we can estimate c_n via

$$
\begin{aligned}
& \int_0^T r_\ell\left(t + \frac{n}{W}\right)\left(s_{1,\ell}^*(t) + \cdots + s_{M,\ell}^*(t)\right) dt \\
= \; & \sum_{k=1}^{L} c_k \int_0^T s_{m,\ell}\left(t + \frac{n}{W} - \frac{k}{W}\right)\left(s_{1,\ell}^*(t) + \cdots + s_{M,\ell}^*(t)\right) dt \\
& + \int_0^T z\left(t + \frac{n}{W}\right)\left(s_{1,\ell}^*(t) + \cdots + s_{M,\ell}^*(t)\right) dt \\
= \; & \sum_{k=1}^{L} c_k \int_0^T s_{m,\ell}\left(t + \frac{n}{W} - \frac{k}{W}\right) s_{m,\ell}^*(t) dt \\
& + \int_0^T z\left(t + \frac{n}{W}\right)\left(s_{1,\ell}^*(t) + \cdots + s_{M,\ell}^*(t)\right) dt \quad \text{(Orthogonality)} \\
= \; & c_n \int_0^T \left| s_{m,\ell}(t) \right|^2 dt + \text{noise term} \quad \text{(Add-and-delay)}
\end{aligned}
$$

$M = 2$ case

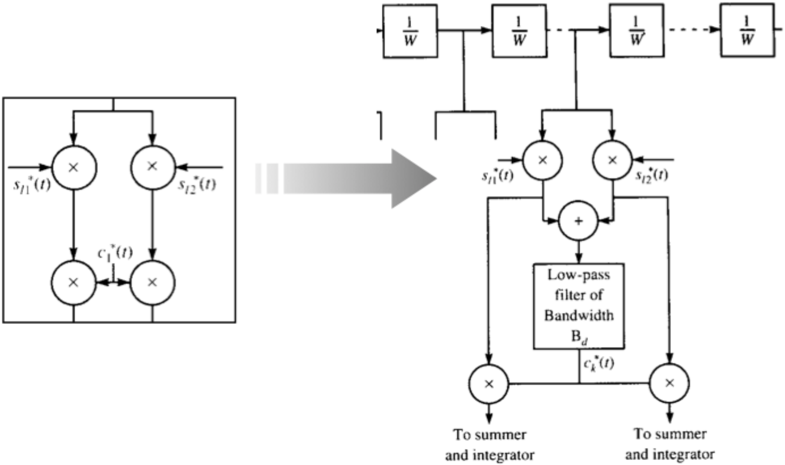

B_d = Doppler spread

Decision-feedback estimator

The previous estimator only works for orthogonal signaling. For, e.g., PAM signal with

$$s_\ell(t) = I \cdot g(t) \text{ where } I \in \{\pm 1, \pm 3, \ldots, \pm(M-1)\},$$

we can estimate c_n via

$$\begin{aligned}
&\int_0^T r_\ell\left(t+\frac{n}{W}\right) g^*(t)dt \\
&= \int_0^T \left(\sum_{k=1}^{L} c_k \cdot I \cdot g\left(t+\frac{n}{W}-\frac{k}{W}\right) + z\left(t+\frac{n}{W}\right)\right) g^*(t)dt \\
&= \sum_{k=1}^{L} c_k \cdot I \cdot \int_0^T g\left(t+\frac{n}{W}-\frac{k}{W}\right) g^*(t)dt + \text{noise term} \\
&= c_n \cdot I \cdot \int_0^T |g(t)|^2 dt + \text{noise term} \quad \text{(Add-and-delay)}
\end{aligned}$$

Final notes

Usually it requires $\frac{(\Delta t)_c}{T} > 100$ in order to have an accurate estimate of $\{c_n\}_{n=1}^{L}$.

Note that for DPSK and FSK with square-law combiner, it is unnecessary to estimate $\{c_n\}_{n=1}^{L}$.

So, they have no further performance loss (due to an inaccurate estimate of $\{c_n\}_{n=1}^{L}$).

What you learn from Chapter 13

- Statistical model of (WSSUS) (linear) multipath fading channels:
  - $c_\ell(\tau;t) = c(\tau;t)e^{-\imath 2\pi f_c \tau}$ and $c(\tau;t) = |c_\ell(\tau;t)|$
  - Multipath intensity profile or delay power spectrum

$$R_{c_\ell}(\tau) \;=\; R_{c_\ell}(\tau;\Delta t = 0)\,.$$

  - Multipath delay spread T_m vs coherent bandwidth $(\Delta f)_c$
  - Frequency-selective vs frequency-nonselective
  - Spaced-frequency, spaced-time correlation function

$$R_{\mathbf{C}_\ell}(\Delta f;\Delta t) = \mathbb{E}\left\{\mathbf{C}_\ell(f+\Delta f;t+\Delta t)\mathbf{C}_\ell^*(f;t)\right\}$$

- Doppler power spectrum

$$S_{\mathbf{C}_\ell}(\lambda) = \int_{-\infty}^{\infty} R_{\mathbf{C}_\ell}(\Delta f = 0; \Delta t) e^{-\imath 2\pi\lambda(\Delta t)} d(\Delta t)$$

- Doppler spread B_d vs coherent time $(\Delta t)_c$
- Slow fading versus fast fading
- Scattering function

$$S(\tau; \lambda) = \mathcal{F}_{\Delta t}\left\{R_{c_\ell}(\tau; \Delta t)\right\}$$

- Jakes' model
- Rayleigh, Rice and Nakagami-m, Rummler's 3-path model
- Deep fading phenomenon
- $B_d T_m$ spread factor: Underspread vs overspread

- Analysis of error rate under frequency-nonselective, slowly Rayleigh- and Nakagami-m-distributed fading channels (≡diversity under Rayleigh) with $M = 2$
  - (Good to know) Analysis of the error rate $\cdots$ with $M > 2$.
- Rake receiver under frequency-selective, slowly fading channels
  - Assumption: Bandlimited signal with ideal lowpass filter and perfect channel estimator at the receiver
  - This assumption results in a (finite-length) tapped-delay-line channel model under a finite delay spread.
  - Error analysis under add-and-delay assumption on the transmitted signals